A synthetic approach to produce recombinant adeno-associated virus (rAAV) in Chinese hamster ovary (CHO) cells

A DISSERTATION

SUBMITTED TO THE FACULTY OF

THE UNIVERSITY OF MINNESOTA

BY

WEN CAI

IN PARTIAL FULFILLMENT OF THE REQUIREMENTS

FOR THE DEGREE OF

MASTER OF SCIENCE

Advisor: Professor Wei-Shou Hu

September 2023

Acknowledgements

I am extremely grateful for the exceptional guidance and mentorship provided by my advisor, Professor Wei-Shou Hu, throughout the course of my master's program. His unwavering support, insightful guidance, and dedication have been instrumental in shaping my academic journey. Professor Hu's commitment to my growth, both professionally and personally, has been a constant source of inspiration. Their expertise and encouragement have not only enriched my understanding of system biology and biotechnology but have also instilled in me a deep appreciation for the pursuit of knowledge and excellence.

I wish to extend my heartfelt appreciation to the remarkable collaborators who have made our joint projects both stimulating and immensely rewarding. I am deeply grateful to Dr. Georgiy Aslanidi, whose guidance has been pivotal in steering our projects towards success and fostering a mindset of innovative thinking. I would also like to extend my gratitude to Dr. Masato Yamamoto from the Medical School at the University of Minnesota. His generosity in providing us with the Ad5-RGD virus and his insightful discussions and unwavering support, have significantly contributed to the advancement of our research endeavors. Furthermore, I am indebted to Dr. Georgiy Aslanidi once again, as well as to Dr. Michael Smanski, for their willingness to devote their time and expertise as members of my committee.

In addition, I would like to extend my sincere gratitude to the members of the Hu group, whose presence has greatly contributed to my academic and personal growth throughout this journey. I really appreciate Min Lu for being a mentor to me and taught me everything about molecular biology and vector designing. Huge thanks to Yu-Chieh Lin, Janani Narayan, Pedram

Motallebnejad, and Han-Jung Kuo for the support and the great times we were to share. I also want to thank all the members of the Hu group, past and present.

Lastly, I want to thank my family. I thank my parents for full and absolute support without adding any pressure.

Abstract

Recombinant adeno-associated virus (rAAV) is one of the most promising gene delivery vectors for somatic gene therapy. Currently, its prevailing manufacturing technologies are relying on transiently transfecting host cells with three plasmids or infection of producer cell lines with helper viruses. Both methods pose real issues in process development, such as difficulty to scale-up or cleaning up helper virus from final products. Commonly used host cell lines for rAAV manufacturing are HEK293, and Sf9. Our lab has previously designed a helper virus-free, plasmid-free, stable cell line production system for rAAV2 via synthetic biology approach. The stable cell line was constructed by integrating multiple copies of rAAV2 genome, AAV2 Cap, AAV2 Rep and Ad5 helper genes which are under inducible promoter control and organized as three separate segments in Genome module, Replication module and Packaging module, into HEK293 cells genome. The stable cell line produced infectious rAAV2 particles upon induction. In this study, we aimed to explore the possibility of using Chinese hamster ovary (CHO) cell as the host cell and creating a stable producer cell line for rAAV2 production. Compared to HEK293 and Sf9, CHO cell holds many advantages. As the most commonly used industrial cell line for therapeutic protein production, it could reach high density in suspension cell culture using serum-free media and is resilient and robust in manufacturing conditions. This study showed that CHO cells were capable of translating AAV2 viral proteins, replicating rAAV genomes, and packaging them into rAAV vector in transient transfection using the Genome, Replication and Packaging modules. Expression of two Ad5 gene, E1A and E1B, could further enhance rAAV titer. E1A and E1B could be stably integrated into the CHO-K1 host cell genome along with the three modules under inducible promoter control. Current producer cell lines had a low productivity and their productivity

appeared unstable. Nevertheless, our study demonstrated the potential of CHO cell lines as a novel production platform for rAAV manufacturing.

Table of Contents

Introduction

Since AAV's initial isolation in 1965, rAAV vector has quickly became one of the most promising gene delivery vectors for somatic gene therapy. Several features make rAAV vectors a popular choice. First, different serotypes of rAAV have different tissue tropism. rAAV is also incapable of replicating itself without coinfection of a helper virus. This prevents unwanted propagation of virus in clinical trials (Samulski & Muzyczka, 2014). Up to date, the regulatory agency has approved several AAV therapies for clinic use. Luxturna was approved in 2017 to treat retinal dystrophy in children and adults. Later, Zolgensma was approved on 2019 for the treatment of spinal muscular atrophy (He et al., 2021), and Elevidys was launched on 2023 for the treatment of children with Duchenne muscular dystrophy (DMD) (Mullard, 2023). As the future of AAV-mediated gene therapy looks increasing promising, new manufacturing challenges distinct from recombinant protein production start to emerge. There is a real increasing demand for innovation in AAV manufacturing technologies.

AAV is a small, nonenveloped virus with a single-stranded DNA (ssDNA) genome. The size of AAV genome is about 5 kilobases in size. It contains two genes, replication gene (*rep*), and capsid gene (*cap*), flanked by inverted terminal repeats (ITRs) at the two ends of the genome (Wu et al., 2010). The gene of interest is placed in between two ITRs for rational design of rAAV vectors. Although the size of AAV genome is small, the AAV genome has three promoters, termed *p5, p19* and *p40*, and generates multiple open reading frame and isoform proteins (Samulski & Muzyczka, 2014). From the *p40* promoter, the *cap* gene encodes three capsid proteins, VP1, VP2, and VP3, and they assemble into the viral capsid at a ratio of 1:1:10 (Gonçalves, 2005). In addition, an assembly-activating protein (AAP) and the membrane-associated assembly protein (MAAP)

are expressed from the *cap* gene. AAP primarily directs nuclear import of capsid proteins and assembly of the mature capsid (Sonntag et al., 2010), and MAAP participates in AAV secretion from host cells (Elmore et al., 2021; Ogden et al., 2019). From the *p5* and *p19* promoter, four different Rep proteins are expressed. The large *rep* proteins, Rep78 and Rep68, act as DNA helicase and strand-specific endonuclease to facilitate AAV genome replication (Tullis Gregory & Shenk, 2000). The small *Rep* proteins, Rep52 and Rep40, are responsible for packaging AAV genome into capsids (King et al., 2001).

For AAV to complete its replication cycle, the presence of helper functions from coinfection of a helper virus is essential. As AAV was discovered during the preparation of adenovirus preparation (Atchison et al., 1965), human adenovirus 5 (Ad5) is one of the most well characterized helper virus for AAV. Ad5 contributes five crucial helper genes that significantly impact AAV replication: E1A, E1B, E2A, E4orf6, and VA RNA. E1A, a pivotal protein regulator, plays a central role in the modulation of viral gene transcription for both Ad5 and AAV. E1A interacts with the AAV p5 promoter's E1A-inducible element, effectively enhancing the transcription of the AAV Rep gene (Chang et al., 1989). Furthermore, E1A engages with several cellular host factors and plays an important role in modulating apoptosis and antiviral response. The two isoforms of E1B play a distinct role in AAV replication cycle. E1B55K forms a complex with E4orf6 to promote AAV second-strand synthesis and facilitate AAV mRNA export from nucleus (Qiao et al., 2002). In contrast, E1B19K does not directly contribute to AAV replication but functions by counteracting the apoptotic effects triggered by E1A gene products (Matsushita et al., 2004). E2A encodes for an important single-strand DNA binding (ssDNA) protein which stimulates AAV genome replication (Ward et al., 1998; Weitzman et al., 1996). Adenovirus VA

RNA, a noncoding RNA molecule, plays a vital role in inhibiting the host cell's antiviral response that leads to a shutdown of protein synthesis, achieved through VA RNA's binding to and subsequent degradation of protein kinase R (PKR) (Vachon & Conn, 2016). In summary, the five helper genes from Ad5, including E1A, E1B, E2A, E4orf6, and VA RNA, collectively orchestrate various stages of the AAV replication process, encompassing transcriptional regulation, genome replication, mRNA export, modulation of apoptotic responses, and evasion of antiviral defenses.

Utilizing the unique characteristics of AAV biology, numerous manufacturing technologies for rAAV vector production have been developed. The most common manufacturing technology for rAAV vector production is the transient transfection of HEK293T cells with three plasmids, one encoding the therapeutic gene flanked by two AAV ITRs, one encoding AAV *Rep* and *Cap* genes, and one containing Ad5 helper genes, E2A, E4 and VA RNA (Clément & Grieger, 2016). The triple transfection technology can produce rAAV vectors in high titer, up to 10^{14} VG/mL, but it also faces challenges of decreased transfection efficiency at large scale and plasmids quality control (Srivastava et al., 2021). To address the issue associated with scaling-up, many studies have dedicated to developing stable producer or packaging cell lines for rAAV by integrating essential AAV and helper genes into the host cell genome. Some studies stably integrated AAV *Rep* and *Cap* gene and rAAV genome into A549 (Farson et al., 2004) and HeLa cells (Chadeuf et al., 2000; Clark et al., 1995) and isolated clones that can produce rAAV vectors by infecting clones with adenovirus. Alternatively, one study integrated Ad E1A/E1B, E2/E4/VA RNA and AAV *Rep*/*Cap* gene into HeLa cell line, attempting to create inducible AAV packaging cell line that did not require subsequent plasmid transfection or helper virus infection (Qiao et al., 2002). Unfortunately, the isolated cell line appeared to be unstable, potentially due to cytotoxicity

from AAV *Rep* proteins (Schmidt et al., 2000) and Ad helper proteins (Qiao et al., 2002). Recently, our lab successfully constructed a stable, plasmid-free, and helper virus-free rAAV producer cell line via a synthetic biology approach (Lee et al., 2022). To resolve potential cytotoxicity from Ad helper proteins and AAV proteins, we controlled the expression of AAV and Ad viral genes by the doxycycline inducible TetON promoter and the Cumate Switch promoter. We stably integrated Ad2 DBP/E4orf6, AAV2 Rep68/Rep52, and rAAV2 genome into E1A-E1B expression HEK293 cells. The isolated cell line is stable after 30 doublings and can produce 10^5 VG/Cell (Min Lu, Personal Communication).

CHO cell lines are the prevailing mammalian host cells used for large scale production of therapeutic proteins. Right now, monoclonal antibodies that are produced in CHO cells made up more than 90% of the therapeutic protein market. The commercial value of CHO produced therapeutic protein exceeds USD $100 billion. Many attributes of CHO cells make them the standard platform for biologics manufacturing. First, advancements in CHO cells culture technology including efforts of optimizing medium design and cell line engineering strategies have pushed protein production in CHO cells to more than 10 g/L (Kim et al., 2012). CHO cells also have excellent post-translational modification characteristics. They generate recombined proteins with corrected glycosylated patterns and folding forms that align well with human and remain biologically active (Kuriakose et al., 2016). Finally, CHO cells can be easily adapted to serum-free and chemical defined media and grow in suspension conditions. Large-scale stirred tank bioreactors, exceeding a capacity of 10,000 L, have been implemented for cultivating suspension cultures of CHO cells (Kim et al., 2012). Included in the CHO products list is viral protein for immunization applications, such as that for respiratory syncytial virus (Swanson et al., 2020) .

Missing from that list is virus for vaccine and gene delivery vector applications. Because CHO cells offer advantages to be easily cultured, achieving rAAV vector production in CHO cells could potentially decrease manufacturing cost. The objective of this study was to evaluate the feasibility of producing rAAV2 particles using CHO cells and explore the potential of developing a stable rAAV2 producer cell line derived from CHO cells.

Material and Methods

VECTOR DESIGN

The rAAV2 genome module was constructed by cloning the rAAV2-GFP genome from pAAV-CAG-GFP (Addgene #37825) into a Leap-In transposon backbone (ATUM, Inc.) with a puromycin resistance gene driven by a phosphoglycerate kinase promoter. The inducible rAAV2 genome module was constructed by replacing the CAG promoter in the rAAV2 genome module with RSV-LacO promoter (Agilent) and linked a *LacI* repressor gene to the puromycin resistance gene. The construction of the replication module (RM) and packaging module (PM) was described in the previous publication. The new RM was a modification of previous RM by the replacement of the GeneSwitch promoter with a TetON promoter (Takara Bio) and the removal of GeneSwitch transactivator gene (Figure 1A) (Lee et al., 2022). Adenovirus 5 (Ad5) E1A gene was amplified from HEK293 cells genome by primer pairs 5’ ctctctggctaactagagaaccactcttgagtgccagcga 3’ and 5’ cctgcacctgaggagtgaaataaacttacatcaactcattcagc 3’ and inserted downstream of the human cytomegalovirus (CMV) immediate-early enhancer and promoter. Ad5 E1B and Ad5 E1B55K genes were amplified from HEK293 cells genome using forward primers 5’ agctgtgaccggcgcctacaacatctgacctcatggagg 3’ and 5’ agctgtgaccggcgcctacagccgccaccatggagcgaagaaacccatc 3’, and reverse primers 5’

cctgcacctgaggagtgaaatcaatctgtatcttcatcgcta 3' and 5' cctgcacctgaggagtgaaatcaatctgtatcttcatcgctag 3' and inserted downstream of the human elongation factor-1α (EF-1 α) promoter. To build pEB1 and pEB2, the E1B or E1B55K gene with the EF-1 α promoter was cloned into a Leap-In transposon backbone with a zeocin resistance gene linked to a reverse tetracycline transactivator gene driven by a phosphoglycerate kinase promoter. To build pEAB1 and pEAB2, E1A and E1B or E1B55K genes with its promoter were assembled into the Leap-In transposon backbone with a zeocin resistant gene. For the construction of inducible helper module pTEAB, E1A coding sequence was first cloned downstream of the TetON promoter. The resulting sequence was amplified by PCR and assembled with the E1B or E1B55K gene with the EF-1 α promoter into the Leap-In transposon backbone with a zeocin resistance gene. pAAV-CAG-GFP (Addgene), pAAV-RC2 (Cell biolab), and pHelper vectors (Cell biolab) were used for triple transfection.

CELL CULTURE AND SINGLE CELL CLONING

CHO-K1 CCL61 cells (ATCC) were cultured in Dulbecco's Modified Eagle Medium/Nutrient Mixture F-12 (DMEM/F12, Gibco) supplemented with 10% Fetal Bovine Serum (Gibco) and 1X antibiotic-antimycotic (Gibco). Stable cell lines were generated by co-transfection of transposon modules with leap-In transposase mRNA (ATUM) at a 1:1 DNA:RNA ratio. After three days of outgrowth, cells were passage into selection media containing puromycin (Invivogen), hygromycin B (Invivogen), blasticidin (Invivogen), and zeocin (Gibco). After two weeks of selection, single cell cloning was performed in 96-wells by limiting dilution. After two weeks of expansion, survived clones were re-seeded in 24-well plates for expansion and titer screening. The workflow was fully described in Figure 5.

rAAV2 PRODUCTION

For rAAV2 production via transient transfection, CHO-K1 CCL61 cells were seeded in 24-well plates at $1.5 * 10^5$ cells per well. One day after seeding, medium with 10 $\mu g/$mL doxycycline and 90 $\mu g/$mL cumate was replaced for induction and the plasmid DNA-lipid complexes prepared from Lipofectamine™ LTX Reagent with PLUS™ Reagent (Invivogen) were added. Cells were harvested four days post seeding. For rAAV2 production via producer cell pool and cell line, cells were seeded in 24-well plates at $1.5 * 10^5$ cells per well. One day after seeding, medium with 10 $\mu g/$mL doxycycline (Sigma Aldrich) and 90 $\mu g/$mL cumate (Sigma Aldrich) was replaced for the culture. Cells were harvested four days post seeding.

rAAV2 CHARACTERIZATION

Harvested cells were lysed by three cycles of freeze/thaw at -80°C/37°C and treated with $\geq$250 units/mL Benzonase (Millipore Sigma E1014) for one hour. Benzonase activity was quenched by adding 2mM EDTA, and cell lysate was centrifuged at 16,000 xg for 10 minutes to remove debris. For physical titration, proteinase K (Macherey-Nagel, 740506) was added to digest rAAV2 capsid and release viral ssDNA. The ssDNA was isolated by column purification (Zymo Research). To measure vector genome titer of samples, qPCR was performed on purified genomes with pAAV-CAG-GFP as a reference standard using the primer pairs against the GFP coding sequence, 5' TTCAAGGACGACGGCAACTAC 3' and 5' TCGATGCCCTTCAGCTCGAT 3'. The transducing titer was measured by RM4 assay cell line (Lee et al., 2023). RM4 assay cells were seeded $1.5 * 10^5$ cells per 24-well with 10 $\mu g/$mL doxycycline and 90 $\mu g/$mL mifepristone

(ThermoFisher Scientific). rAAV lysates were added to the cultures one day post seeding, and transducing titers were measured two days post transduction.

REAL-TIME AND QUANTITATIVE PCR

Intracellular genomic DNA (gDNA) and RNA were extracted by Quick-DNA/RNA Miniprep (Zymo Research) according to its manufacturer's instruction, and on column DNase digestion was performed by RNase-Free DNase Set (Qiagen). Messager RNA (mRNA) was reversed transcribed into complementary DNA (cDNA) via SuperScript III First-Strand Synthesis SuperMix Kit (Invitrogen). For the calculation of relative gene expression, *Gadph* was used as reference gene, while *Vinculin* (*Vcl*) was used as the reference gene for the calculation of integrated gene copy number. The primers used in the assay were designed and synthesized by Integrated DNA Technologies (IDT).

WESTERN BLOTTING

Harvested cells were lysed by NP-40 cell lysis buffer containing protease inhibitor (Complete Mini, Roche). Cell lysates were clarified by centrifuging the sample under 4 ℃ at 15,000 rpm for five minutes. Proteins were heat-denatured by 4X Bolt™ LDS Sample Buffer (Invitrogen) and 10X Bolt™ Reducing Agent (Invitrogen). The same amount of total cell lysates (10 μg per lane) along with Novex™ Sharp Pre-stained Protein Standard (Invitrogen) were loaded on the Bolt™ Bis-Tris Plus Mini Protein Gels (Invitrogen). After transferring proteins to the 0.45 μm nitrocellulose membrane (Bio-Rad), the blots were blocked overnight with the 5% non-fat dry milk powder. Capsid proteins were detected and stained with primary anti-AAV VP1/VP2/VP3 antibodies (Progen, #65158) and corresponding secondary alkaline phosphatase (AP)-conjugated

antibodies (diluted 5000 folds in 5% NFDM). The chemiluminescent signal was detected using the Immun-Star™ AP Chemiluminescence Kits (Bio-Rad).

ADENOVIRUS GENERATION AND TITRATION

Ad5-RGD virus was generated in HEK293 cells by virus propagation. HEK293 cells were seeded in the 10 cm dish at a density of 8.8 x 10^6 cells/dish for 24 hours before infection. Cells were cultured in Dulbecco's Modified Eagle Medium (DMEM, Gibco) supplemented with 5% Fetal Bovine Serum (Gibco) and 1X antibiotic-antimycotic (Gibco). Ad5-RGD virus stock from Prof. Masato Yamamoto was used to infect each 10 cm dish at a MOI of 3 for 2 days. Cells were harvested upon display full cytopathic effects (CPE). Virus was released by three rounds of freeze thaw cycles and virus lysate was stored in -80 ℃.

FROG VIRUS 3 GENERATION AND TITRATION

Frog Virus 3 (FV3) was generated in BHK-21 baby hamster (*Mesocricetus auratus*) kidney cells by virus propagation. BHK-21 cells were seeded in 10 cm dish at a density of 4.0 x 10^6 cells/dish for 24 hours before infection. Cells were cultured at 30 ℃ in Dulbecco's Modified Eagle Medium (DMEM, Gibco) supplemented with 10% FBS (Gibco) and 1X antibiotic-antimycotic (Gibco). FV3 virus stock was used to infect each 10 cm dish at a MOI of 0.1 for 5 days until cells were complete lysed. Virus was harvested by three rounds of freeze thaw cycles and virus lysate was stored in -80 ℃.

PLAQUE ASSAY FOR DETERMINING INFECTIOUS FV3

BHK-21 cells were seeded in 6-well plate at a density of 4.0 x 10^5 cells per well at 37 ℃ for 24 hours. Six rounds of ten-fold serial dilution of FV3 virus lysate was made in DEME supplemented with 2.5% FBS at a total volume of 1.2 mL. Two replicates of diluted sample (1 x 10^{-3} to 1 x 10^{-5}) were added at a volume of 100 μL per well on each plate. After incubating under room temperature with gentle sharking for 1-2 hours, the inoculum was discarded and DMEM supplemented with 1% methylcellulose was added per well at a volume of 3 mL. The plates were incubated under 30 ℃ for 6 days. After 6 days, cell monolayer was stained with 0.1% crystal violet and FV3 titer (PFU/mL) was determined by counting the number of isolated plaques in each well on an illuminated surface.

Results

1 Transient rAAV2 Production in CHO Cells

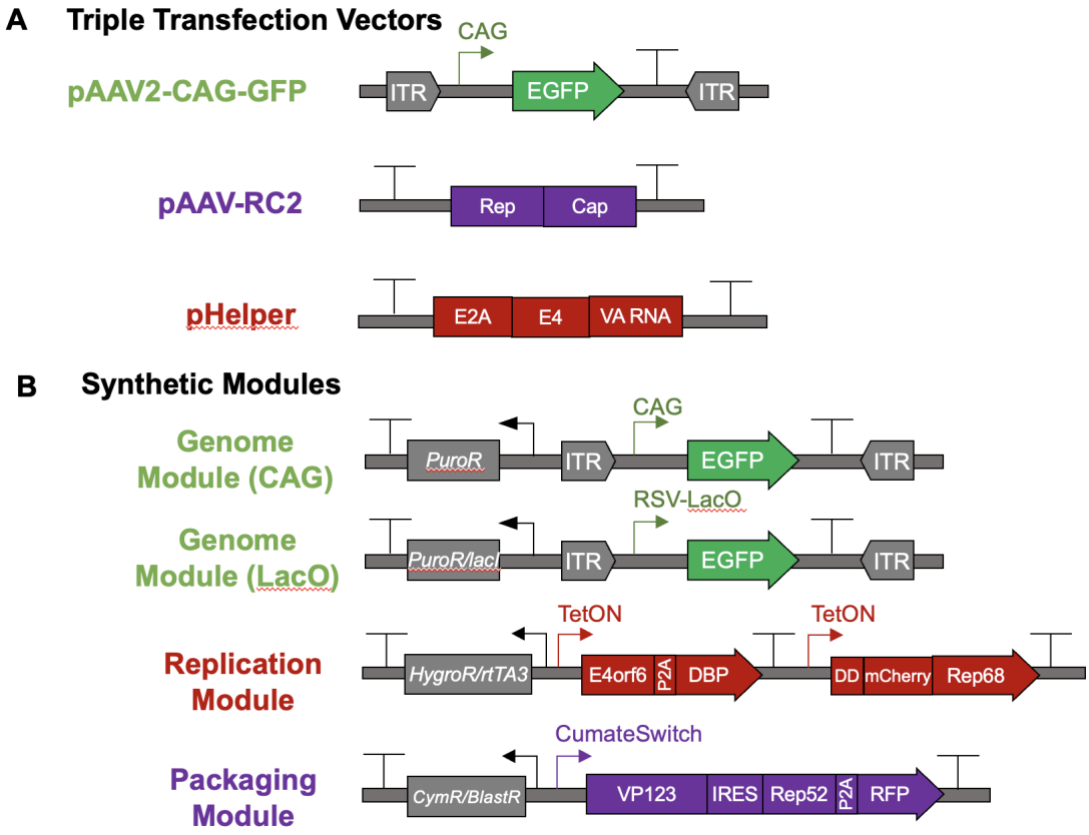

Figure 1. Schematic diagrams of traditional vectors for triple transfection technology and the synthetic modules used of this study. (A) Gene modules of three traditional vectors for triple transfection technology. (B) Gene modules of four synthetic modules. Symbols: CAG denotes the CMV early enhancer/chicken β actin (CAG) promoter; LacO denotes the lactose (lac) operator; RSV denotes the Rous sarcoma virus promoter; ITR denotes the inverted terminal repeats; rtTA3 denotes the reverse Tet trans-activator gene; CymR denotes the Cym Repressor; DD denotes the destabilization-domain; P2A denotes the 2A self-cleaving peptides; IRES denotes the internal ribosome entry site.

We initially investigated whether CHO-K1 cells could transiently produce infectious rAAV2 particles using two sets of vectors. The triple transfection vectors are traditionally used for the production of rAAV by transient transfection and continue to be one of the most widely employed rAAV manufacturing technologies (Figure 1-A). Among the three DNA plasmids, one

contains the gene of interest (GOI) that is flanked by two AAV inverted terminal repeat sequences (ITRs)—in our case, the GOI was represented by enhanced GFP (eGFP). The second plasmid contains the native reading frames and promoters of AAV *Rep* and *Cap* genes. The third plasmid contains three helper factors from human adenovirus 2 (Ad2), E2A, E4 and VA RNA. The E2A gene encodes a single-strand DNA binding proteins (ssDBP) which binds AAV genome during its replication process. E4orf6 protein, which is one of the protein isoforms encoded by the E4 gene, is responsible for AAV mRNA export from the nucleus by forming a complex with E1A55K. The E1B55K/E4orf6 complex also triggers degradation of host cellular proteins, including p53 and MRN complex. VA RNA is a noncoding RNA (ncRNA) which mediates the degradation of protein kinase PKR and blocks PKR-triggered protein synthesis shutdown.

The AAV2 native promoters within the three synthetic modules, namely the genome module (GM), packaging module (PM), and replication module (RM), were substituted with inducible promoters (Figure 2B). AAV2 genes and Ad5 helper genes were rearranged into RM and PM based on their functions (Figure 1-B). Rep68 coding sequence (CDS) was linked with a destabilization domain (DD) to control the cytotoxicity from leaky expression. It was then cloned into the replication module under the control of Tet-ON promoter. E4orf6 CDS from E4 gene and DBP CDS from E2A gene were cloned out and linked together with a self-cleaving peptide (P2A). The whole sequence was cloned into the replication module under Tet-On promoter. For the packaging module, intron was removed from the native AAV2 *Cap* gene sequence because previous data suggested VP1/2/3 transcripts were not properly spliced. The start codon for VP1 CDS was mutated from ATG to ACG. Rep52 CDS was cloned out and linked to VP123 CDS with

an internal ribosomal entry site (IRES). The C terminal of Rep52 was linked with a P2A and red fluorescent protein. VA RNA was not included in current synthetic constructs (Lee et al., 2022).

A

Plasmids	Transducing Units (TU/mL)
Traditional Vectors	$2.1 \pm 2.0 * 10^3$
Synthetic Modules (+10D90C)	$1.2 \pm 0.2 * 10^4$
Synthetic Modules (-10D90C)	Undetectable

B

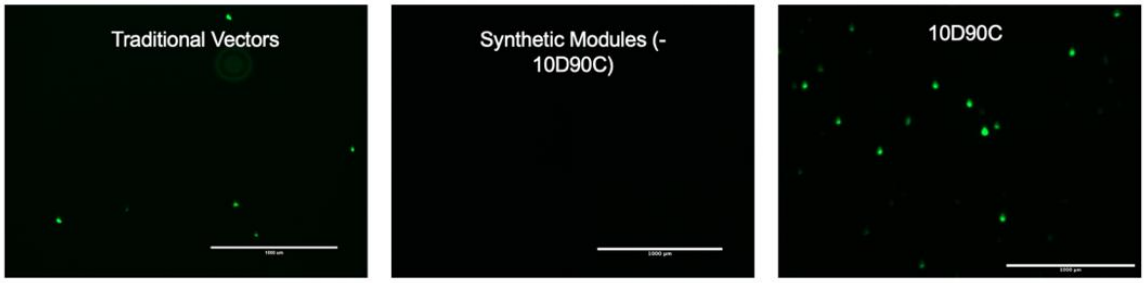

Figure 2. Transient transfection production of rAAV2-GFP by traditional vectors or synthetic modules in CHO-K1 cells. (A) Transducing units (TU) at 72 hpt. The synthetic module transfection was performed with or without induction by 10 μg/mL of doxycycline and 90 μg/mL cumate (10D90C). (B) GFP fluorescence images of RM4 assay cells at 48 h after being transduced with rAAV2-GFP in the cell lysate of three cultures in (A).

To test its capability of producing rAAV, CHO-K1 cells were seeded at 4 x 10^4 cells/cm^2 for 24 hours, before 10 μg/mL of doxycycline and 90 μg/mL cumate (10D90C) were added and plasmid transfection was performed. Three days after transfection, cell pellets were harvested, and freeze thaw cycles were performed to extract rAAV2-GFP particles. The quantity of infectious rAAV2-GFP particles in the freeze-thaw cell extract was assayed using the RM4 cells. The RM4 cell line was an assay cell line for the titration of infectious rAAV2-GFP particles. It was constructed in our laboratory by integrating the replication module into the host HEK293 cell

genome to render it the capability of replicating DNA segments flanked by AAV2 ITR. When assay cells were induced and infected with rAAV2-GFP particles, the GFP gene would amplify along with rAAV genome and express a high GFP signal that was detectable. The number of GFP-positive cells can be quantified as a measure under fluorescent microscopy or through flow cytometry.

The results from the assay cell line demonstrated that transiently transfecting CHO-K1 cells with either traditional vectors or synthetic modules resulted in the production of transducible rAAV2-GFP particles. Transient expression of traditional vectors in CHO-K1 produced 2.1 x 10^3 TU/mL, while transient expression of induced synthetic modules produced 1.2 x 10^4 TU/mL. In the case of transfection with synthetic modules, induction of *rep*, *cap* and helper genes with doxycycline and cumate inducers yield more infectious rAAV2-GFP particles than without induction (Figure 2).

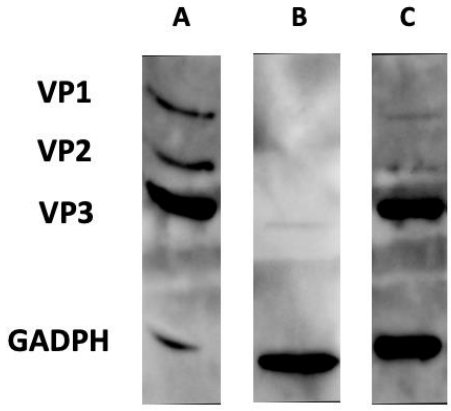

Figure 3. Western blot analyses of adeno-associated virus (AAV) Cap protein expression in HEK293 (A) or CHO-K1 CCL61 cells (B and C). Lane (A) transient transfected HEK293 cells by three traditional plasmids at 72 hpt. Lane (B) transient transfected CHO-K1 cells by three induced synthetic modules at 24 hpt. Lane (C) transient transfected CHO-K1 cells by packaging module only at 24 hpt. GADPH was used as a loading control.

The expression of AAV2 *cap* proteins in transiently transfected CHO-K1 cells at 24 hours post-transfection (hpt) was evaluated by western blotting using anti-AAV VP1/VP2/VP3 antibody (Figure 3). GADPH was used as loading control. CHO-K1 cells were transfected with three synthetic modules and induced by 10D90C (Lane B). To clearly observe *Cap* gene expression pattern, packaging module was transfected into CHO-K1 cells alone and induced with 90 μM cumate (Lane C). The sample of HEK293 cells transfected with three traditional vectors and harvested at 72 hpt was used as positive control (Lane A).

Four rows of bands were detected on the membrane. One row of bands was between 30 kDa and 40 kDa and matched the molecular weight of GADPH. The positions of GADPH bands from HEK293 and CHO-K1 samples were horizontal to each other. Two CHO-K1 GADPH bands were the same size, while the HEK293 GADPH band was smaller compared to CHO-K1 samples. The rest three rows of bands were positioned between 60 kDa and 110 kDa, with two rows of bands in between 60 kDa and 80 kDa, and one row of bands in between 80 kDa and 110 kDa. The molecular weight pattern of three bands matched with three isoforms of AAV2 *Cap* protein, VP1, VP2 and VP3. VP3 band was the largest in size, and sizes of VP1 and VP2 bands were similar to each other. Bands of VP1, VP2, and VP3 were clearly imaged for lane A and lane C. For lane B, only VP3 band was faintly detected. Due to the much lower concentration of VP1 and VP2 proteins compared to VP3, the absence of bands for VP1 and VP2 in lane B could be attributed to the assay's sensitivity. However, this result also suggested that when overexpressing three synthetic modules, three capsid proteins were expressed in low abundance.

Many gel densitometry and mass spectrometry studies on wild type AAV capsids have demonstrated that the benchmark ratio between VP1, VP2, and VP3 was 1:1:10 (Gonçalves, 2005).

For the positive control in HEK293, the ratio between three capsid proteins was similar to its benchmark value. Interestingly, however, transient expression of three capsid proteins in CHO-K1 showed a ratio deviated from the benchmark value. One possible explanation for this was we have previously mutated the first start codon in Cap reading frame from ATG to ACG (Figure 3) (Lee et al., 2022).

The results presented above demonstrated that it is possible to make CHO cells' produce rAAV2 vectors, even though the productivity was very low. Triple transfection on suspension HEK293 cells could yield 10^{11} to 10^{12} VG/mL and 10^{8} to 10^{9} TU/mL (Grieger et al., 2016), but transfection of same plasmids to CHO-K1 could only generate 10^{3} transducing units per mL (TU/mL).

The transient transfection results also showed that CHO-K1 produced 10 folds of more infectious rAAV2-GFP particles using synthetic modules than using traditional vectors. A key difference between the two systems was that, while the traditional vector used a native promoter of AAV. The synthetic system used inducible promoters. CHO cells are not natural host cells for either AAV or adenoviruses, therefore it is possible that AAV promoters were more susceptible to suspension by CHO's antiviral response than those inducible promoters and could not efficiently initiate transcription. On the contrast, the backbone of Tet-On expression system and cumate gene-switch are the EF1-α promoter and CMV promoter. Regardless, these results suggested the potential of expressing all AAV2 viral component and produce rAAV2 in CHO-K1 cells.

1.1 Human adenovirus 5 (Ad5) E1 Gene Enhanced Transient rAAV2 Production.

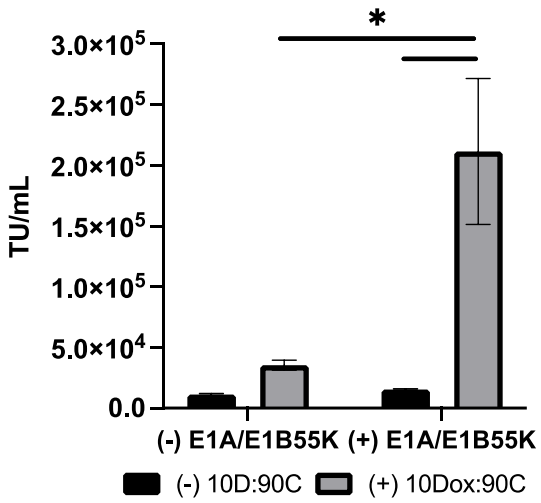

Figure 4. Transient expression of E1A and E1B-55K genes increased rAAV2 transducing titers. CHO-K1 cells were transiently transfected with GM, RM, and PM with (+E1A/E1B55K) or without E1A and E1B-55K (-E1A/E1B55K). Transfectants were induced (+10D90C) or un-induced (-10D90C) for 72 h before harvest. Virus titers were measured by the assay cell line RM4 by counting the GFP-positive cells from twelve images. Data represents mean and standard deviation of three independent replicates. *: $p < 0.05$, **: $p < 0.01$, ***: $p < 0.001$ as determined by a two-way analysis of variance (ANOVA) test.

Many studies have discussed the regulatory role of Ad5 E1 gene in AAV replication. E1B55K forms a helper factor complex with E4orf6 to facilitate with DNA replication and mRNA export from nucleus, and E1A is believed to activate *p5* and *p19* promoters and transform intracellular environment to become more suitable for viral DNA replication (Matsushita et al., 2004). The most widely used cell line in rAAV production, HEK293 cell line, naturally contained E1 gene of human adenovirus 5. It was transformed by exposing human embryonic kidney cells to hAd5 sheared fragments. Following the transformation, the E1 gene-containing segment of the

hAd5 genome was integrated into human embryonic kidney cells, as previously demonstrated. Consequently, CHO cells lack the E1 gene.

To assess whether inclusion of the E1 gene could enhance rAAV production in CHO cells, two plasmids were employed, containing Ad5 E1A and Ad5 E1B55K genes, regulated by the EF1-α promoter. These plasmids, along with the three synthetic modules (GM, PM, and RM), were transfected into CHO-K1 cells and induced with 10D90C to produce rAAV2 particles. Cell pellets were harvested 72 hpt and RM4 cell line was used for titer evaluation. The results were compared to transient transfection of three synthetic modules alone with induction in CHO-K1. Results from the assay cell line showed that, upon induction, transfection of three synthetic modules with Ad5 E1A and E1B55K produced 2.0 x 10^5 TU/mL. The titer was 4-5 times more than transfection of three synthetic modules without E1A and E1B55K (Figure 4).

2 Establishment of Stable CHO Cell Pools Producing rAAV2

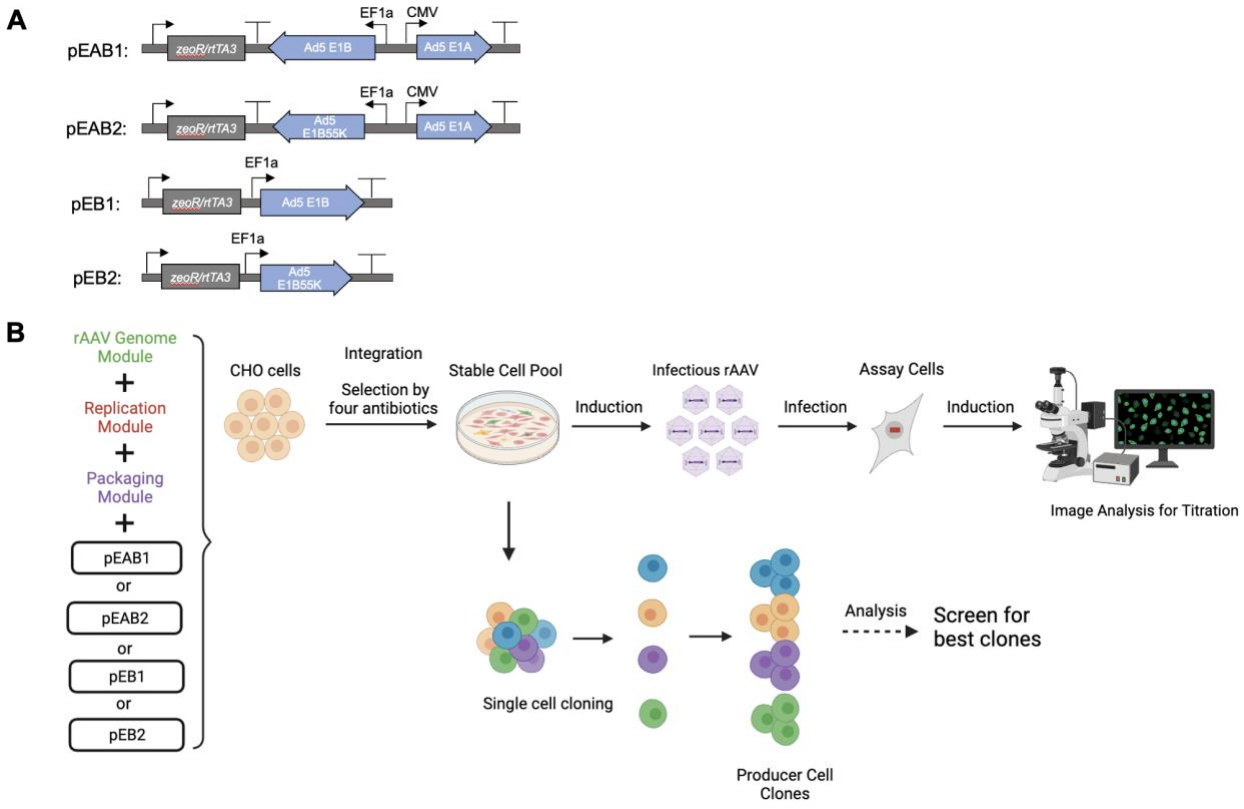

Figure 5. Construction and characterization of stable cell pools. (A) Gene modules of four helper modules. Symbols: EF1α denotes the human elongation factor 1-α promoter; CMV denotes the human cytomegalovirus immediate-early enhancer and promoter; Ad5 denotes the human adenovirus type-5; E1A denotes the coding sequence of adenovirus early region 1A; E1B denotes the coding sequence of adenovirus early region 1B; E1B-55K denotes the coding sequence of E1B isoforms, E1B 55kDa protein; ZeoR denotes zeocin resistance gene. (B) Schematic diagram of four stable producing cell pools construction.

Since our data had demonstrated expression of E1 gene products improved rAAV titer in CHO-K1 by transient transfection, we proceeded to integrate both E1A and E1B gene along with the three synthetic modules into CHO-K1 genome to construct a CHO-K1-derived stable producer cell line. Four helper modules, pEAB1, pEAB2, pEB1 and pEB2, with transposon sequences and the zeocin selective marker were designed and constructed. Ad5 E1B gene encodes for two isoforms, E1B55K and E1B19K. Literature has reported E1B19K and E1B55K have distinct roles

in supporting AAV replication. The known function of E1B19K was that it could enhance rAAV titer by suppressing the apoptotic effect of E1A, while E1B55K facilitates with exporting of viral mRNA from the nucleus. One of my design aims was to include only the minimal set of essential helper genes in the final synthetic modules for integration. Two versions of E1B were used, one has the complete E1B CDS, and the other has only the coding sequence of E1B55K. Each version was further tested for two cases, with or without the co-presence of E1A to evaluate the essentiality of E1A. Hence, a total of four helper modules, pEAB1, pEB1, pEAB2, and pEB2, were constructed (Figure 5-A). The expression of Ad5 E1A was placed under the control of the constitutive promoter, human cytomegalovirus (CMV) promoter with its immediate early enhancer. The expression of Ad 5 E1B was placed under the control of the constitutive promoter, the human elongation factor-1 α promoter (Figure 5-A).

A transposon-based system was adopted to construct stable cell pools. The GM, RM, PM, and one of the four HMs, pEAB1, pEAB2, pEB1 or pEB2, with transposon mRNA were transfected into CHO-K1 cells in 6-well plate. After transfection, cells were grown for three days. Prior to selection, cells were divided into one 100 mm dish and serial diluted by a factor of 2 between wells in a 6-well plate. Cells in both 100 mm dish and 6-well plate were subjected to selection with puromycin (8 nM), hygromycin (400 nM), blasticidin (10 nM), and zeocin (200 nM) for two weeks to obtain four stable cell pools (Figure 5-B).

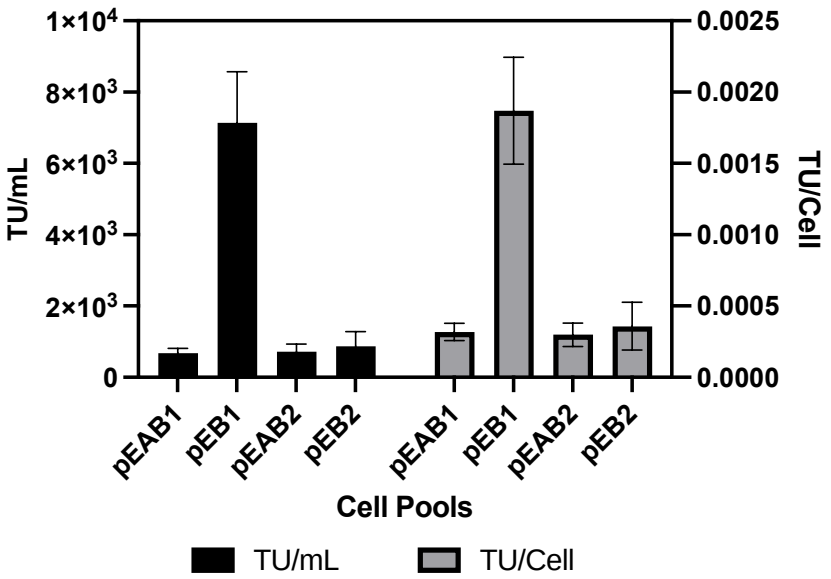

Figure 6. Virus titer obtained through the induction of four stable cell pools. Virus titers were measured by the assay cell line RM4 by counting the GFP-positive cells from twelve images. Data represent mean and standard deviation of three independent replicates.

An interesting observation during cell pool selection process was that the two cell pools with E1B genes proliferated much faster than the two cell pools with both E1A and E1B genes. At the end of selection process, only a few colonies were obtained from the two E1A-E1B cell pools, but the two E1B cell pools became confluent in both the 100 mm dish and 6-well plate. In subsequent culture of those cells, concentrations of all selection markers were reduced by half.

After two weeks of selection, the transducing titers of four cell pools were measured by RM4 assay cell. Virus titers of four cell pools were vastly different. The best producing cell pool was the cell pool integrated with the helper gene E1B, which could produce 7 x 10^3 TU/mL or 0.002 TU/cell. Unexpectedly, two cell pools that were integrated with both E1A and E1B helper genes produced very few infectious rAAV2-particles (Figure 6).

2.1 Loss of Helper Module in Cell pools Previously Integrated with Constitutively E1A and E1B

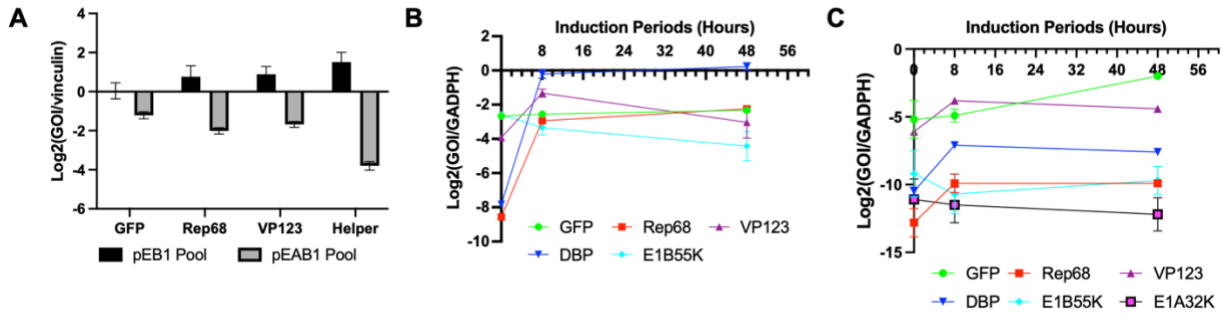

Figure 7. Integrated gene copy number and viral transcript level of four stable cell pools. (A) Copy numbers of GM, RM, PM and HM integrated in the genome. (B) Relative transcript levels of viral genes of cell pool pEB1 before and after induction by dox and cumate. (C) Relative transcript level of viral genes of cell pool pEAB1 before and after induction by dox and cumate. Data represent mean and standard deviation of triplicate qPCR wells. Genome copy was assayed by qPCR of GFP.

We measured the copy numbers of each module integrated into the CHO-K1 genome and the transcript level of key viral genes by qPCR. We tested one cell pool integrated with E1B and one cell pool integrated with E1A and E1B. The best producing cell pool, pEB1, had ~2 copies of genome module, ~4 copies of replication and packaging module, and ~8 copies of helper module. Strikingly, the pEAB1 cell pool had only on ~1 copy of genome module in the host genome, and integrated replication, packaging and helper modules were almost undetectable by qPCR (Figure 7-A).

Our lab has previously integrated the three synthetic modules into HEK293 cells and isolated high producer clone, the GX2 clone. GX2 had ~24 integrated copy number of genome, packaging and replication modules and could produce 5.0 x 10^7 TU/mL (Min Lu, Personal Communication, 2023). Compared to GX2, the cell pool pEB1, derived from CHO-K1 cells,

showed virus titers that were 10,000 times lower. One potential explanation for this discrepancy was that the cell pool pEB1 had fewer integrated copies of the synthetic modules. Specifically, the replication and packaging module copy counts were 6 times lower in pEB1 than in GX2, while the genome module copy count was 12 times lower in pEB1 than in GX2. This information suggested that one strategy to enhance virus titer could involve increasing the copy numbers of viral genes (Figure 7-B).

Profiling of viral transcript level at 8 and 48 hours after induction by qPCR also indicated that the helper module was selected out in the cell pool integrated with E1A and E1B. Induction of pEB1 cell pool increased the expression of DBP, VP123, and Rep68 up to 4 to 8 folds. The transcript level of DBP was comparable to the housekeeping gene GADPH. The transcript levels of VP123, Rep68, and E1B55K were 3 to 4 folds lower than GADPH. In pEAB1 cell pool, the transcript levels of GFP, VP123, DBP, and Rep68 showed 3 to 5 cycle numbers increase upon induction, but the cycle numbers for E1A32K and E1B55K were below an acceptable level. Considering the slow cell growth during selection and the loss of helper module and helper gene expression in E1A-E1B cell pool, it is plausible that expression of E1A was highly cytotoxic and many cells in the pool had lost at least one of the E1A or E1B.

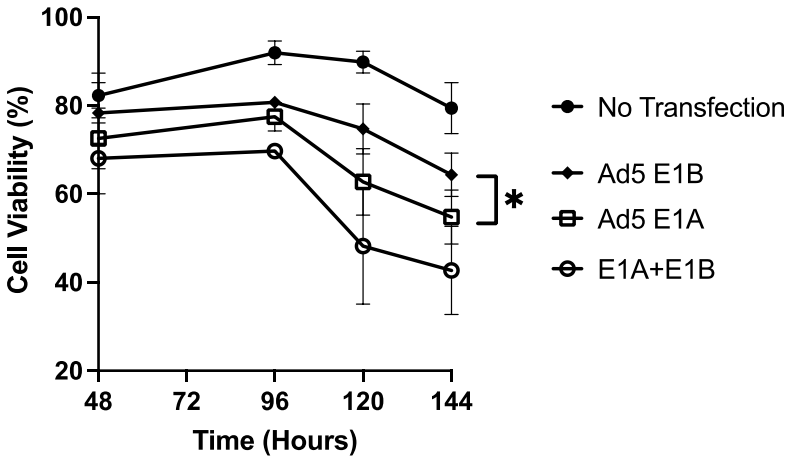

Figure 8. Cell viability of cells transfected with Ad5-E1A (•), Ad5-E1B (■), E1A and E1B (o) and non-transfected cells (•). Cell viability was determined by trypan blue exclusion. Data represents mean and standard deviation of three independent replicates. *: $p < 0.05$, **: $p < 0.01$, ***: $p < 0.001$ as determined by an unpaired, two-tailed, two-sample t-test.

Ad5 E1A or E1B under the promoter EF1-α was transiently transfected into CHO-K1 cells. Cell viability was measured over time to validate whether E1A was damaging to CHO cells. CHO-K1 cells were seeded one day before transfection with E1A and E1B. Viability was measured by trypan blue exclusion using an automated cell counter. As can be seen in Figure 8, E1B transfection allowed cells to maintain a higher viability than in E1A or E1A and E1B transfection. Cells integrated with E1B was observed to grow and multiply rapidly, suggesting that E1B gene products were not cytotoxic. Therefore, E1B-transfected cells were used as a control for potential cytotoxicity from transfection reagents and process. While the viability of non-transfected cells stayed relatively high, viabilities of E1A-transfected, E1B-tranfected, and E1A/E1B-transfected cells started to drop further after 96 hpt. At 48 hpt, the viabilities of non-transfected cells and E1B-transfected cells were 82% and 78%. In comparison to the two groups, the viabilities of E1A-tranfetced and E1A/E1B-transfected cells were lower, down to 73% and 68%. At 120 hpt, about 75% cells were viable for E1B-transfected group, but only 63% and 48% cells were viable for

E1A-transfected and E1A/E1B transfected groups. At 144 hpt, the viability of E1B-transfected cells dropped to 64%, and the viability of E1A-transfected cells and E1A/E1B-transfected cells dropped to 55% and 43%. A paired sample t-test showed that cell viability of E1A-transfected cells was decreasing in a rate statistically significantly faster than the E1B-transfected cells, which supported our previous conclusion that E1A was toxic to CHO-K1 cells (Figure 8).

2.2 Low Level of rAAV2 Genome Amplification in CHO.

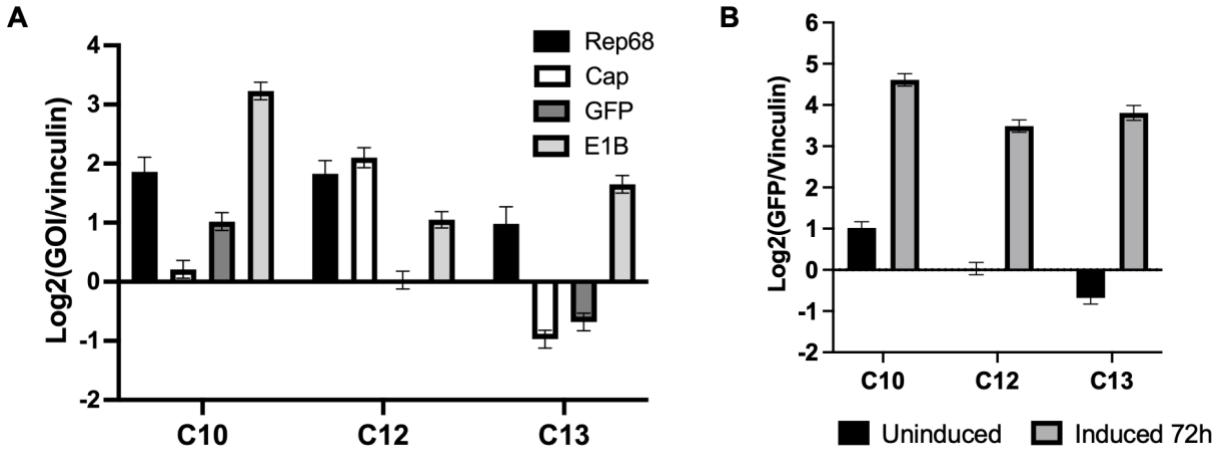

Figure 9. Genomic profiles and fold amplification of three clones, C10, C12, and C13. (A) Copy numbers of GM, RM, PM and HM integrated in the genome. (B) Total genome copy (packaged and unpackaged) before induction and 72 hours after induction. For A-B, data represent mean and standard deviation of triplicate qPCR wells.

We proceeded with performing single cell cloning on cell pool pEB1 by limiting dilution in 96-well plate. In total, forty 96-well plates were seeded, and 65 clones were isolated and screened for rAAV2 production using the RM4 assay cell line. However, initial screening result showed that none of the isolated clones produced infectious rAAV2 particles. We chose three clones and quantified their rAAV2 genome copy and viral transcriptomic profiles.

The copy number of four modules in the genomes of three clones varied certain degree. In general, all four modules were present in all three clones, as assayed by the probe for each module. Replication module and helper module were present at higher copy numbers among three clones, with about 4 copies or more copies per cell. Copy numbers of packaging module varied in the greatest extent between clones, and copy numbers of genome module on average was the lowest. Clone C13 had only ~1 copy of packaging and genome modules. Clone C12 had ~8 copied of packaging module and ~2 copies of genome module. Clone C10 had ~2 copies of genome module and ~4 copies of packaging module (Figure 9-A).

Cells were induced with 10D90C, and the degree of genome amplification was measured. Clone C13 achieved the highest fold (~16 folds) of genome amplification. In comparison, an rAAV-producing cell line from our lab showed that rAAV2 genome produced >1000-fold amplification in HEK293 (Citation). This finding implies that the low degree of genome amplification hampered rAAV2 packaging and production by CHO cells (Figure 9-B).

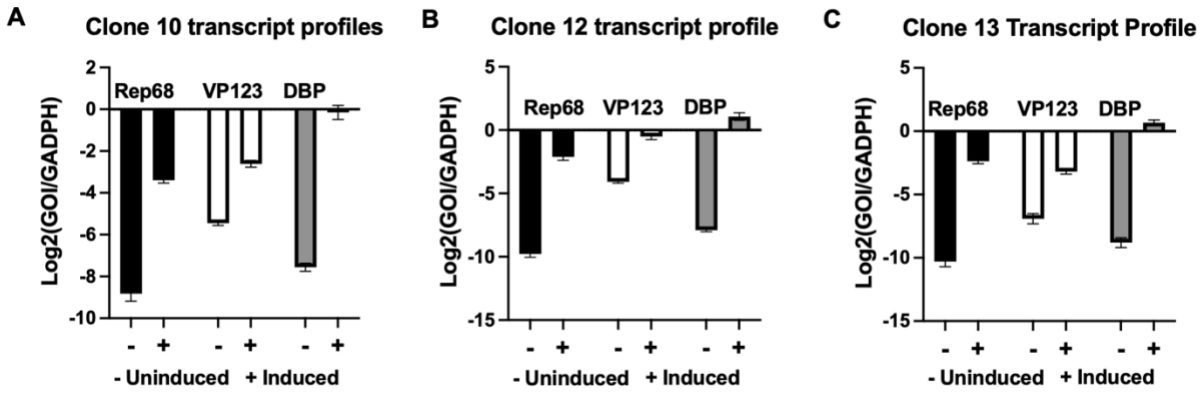

Figure 10. Transcript profiles of three clones, C10 (A), C12 (B), and C13 (C). Transcript level of Rep68, VP123, and DBP were measured before (-) induction and 72 hours after induction (+). Data represent mean and standard deviation of triplicate qPCR wells.

Level of transcripts of three AAV viral genes, Rep68, DBP, and VP123, increased upon induction. DBP transcript levels of three clones were comparable to GADPH after cells were induced for 72 hours. The transcript of DBP in GX2 cells were also highest among all viral transcript encoded in the modules. VP123 and Rep68 transcript levels were one to four folds lower than GADPH (Figure 10). Despite having lower integrated copies of GM, RM and PM, levels of VP123 and Rep68 transcripts were comparable to the high producer cell clone, GX2. DBP transcript level was 1 to 2 folds lower than the DBP transcript level in GX2 (Min Lu, personal communication, 2023).

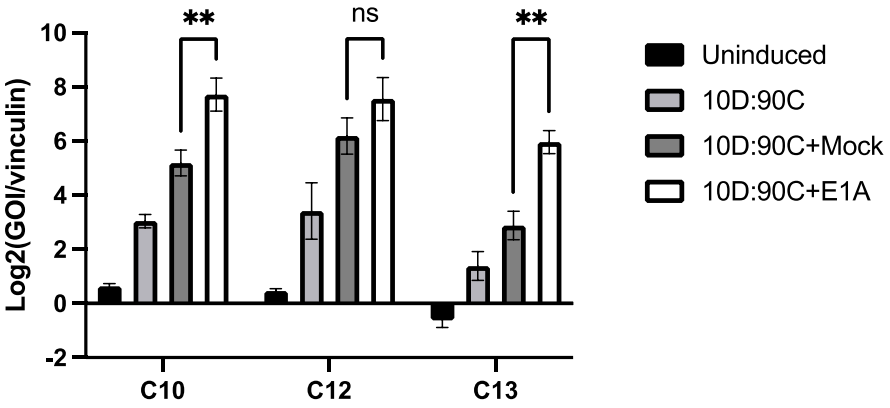

Figure 11. The effects of Ad5 E1A on rAAV2 genome amplification. Three clones were induced with 10D90C. Addition of transfection reagents and transient transfection of E1A was performed at the time of induction. Data represents mean and standard deviation of three independent replicates. *: $p < 0.05$, **: $p < 0.01$, ***: $p < 0.001$ as determined by an unpaired, two-tailed, two-sample t-test.

E1A had been shown to enhance Ad5 genome replication and rAAV2 production. We hypothesized that E1A would have an enhancement role on rAAV2 genome replication. A plasmid containing E1A under EF1-α promoter was introduced into the three clones via transfection. Three clones were induced simultaneously for three days before genomic DNA was isolated. Genome amplification of the E1A-transfected group was compared to three control groups, uninduced cells,

induced cells, and induced cells added with DNA transfection reagents (the mock group). With addition of DNA transfection reagents, genome fold amplifications of three clones went 1-2 cycle number higher than the induced group, but transfection of E1A further increased intracellular genome amplification for 2-4 cycle number. Among three clones, this change of genome amplification two clones was statistically significant. Hence, the results show that E1A was likely had a positive effect on genome amplification.

3 Construction and characterization of stable cell pools.

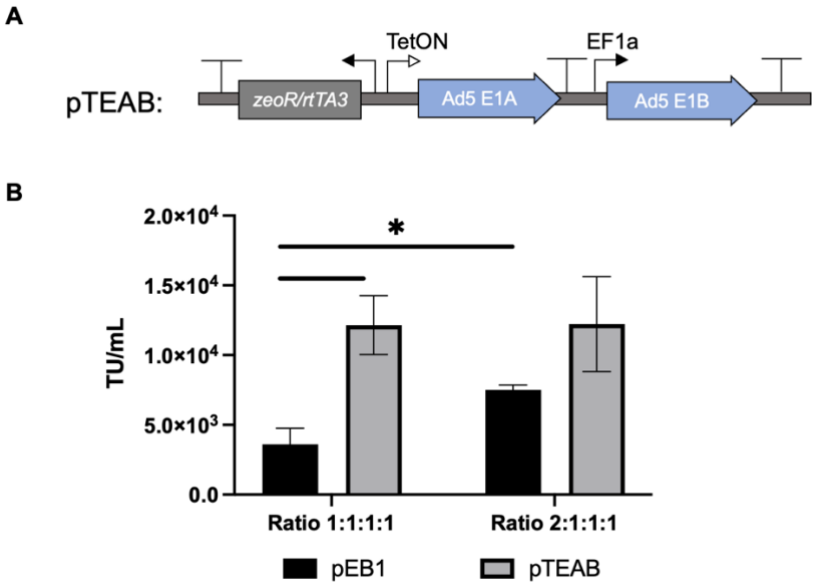

Figure 12. (A) Inducible helper module: pTEAB. (B) Transducing titer of rAAV2 obtained by transient transfection of CHO-K1 cells with GM, PM, RM, the helper module pEB1 or the helper module pTEAB. For B, data represents mean and standard deviation of three independent replicates. *: $p < 0.05$, **: $p < 0.01$, ***: $p < 0.001$ as determined by a two-way analysis of variance (ANOVA) test.

To alleviate E1A's cytotoxic effects, we constructed a new helper module with inducible E1A and constitutively expressed E1B. The CDS of E1A sequence was placed downstream of the Tet-ON promoter, while the expression of Ad5 E1B sequence was under the control of the

constitutive promoter EF1a (Figure 12-A). Three synthetic modules with the new inducible helper module, pTEAB, or the E1B-only helper module, pEB1, were transient transfected into CHO-K1 cells. Transfection was performed one day post seeding and cells were induced with 10 μg/mL doxycycline and 90 μg/mL cumate. Three days after induction and transfection, 1.3 x 10^4 TU/mL was produced. A control transfected with pEB1, and the three synthetic modules produced 4.0 x 10^3 TU/mL (Figure 12-B). The 3-fold titer difference affirmed our previous results that Ad5 E1A enhanced rAAV2 genome amplification in CHO-K1 cells.

Genome amplification was insufficient for rAAV2 production in CHO-K1 cells, we explored the effect of increasing the proportion of genome module in the transfection. Results from RM4 cell line showed that when cells were transiently transfected with the E1B-only helper module and three synthetic modules, doubling the molar ratio of GFP genome increased rAAV2 transducing titer by roughly 2-fold (Figure 12-B). Strikingly, however, when cells were transiently transfected with the inducible helper module with both E1A and E1B and three synthetic modules, doubling the molar content of GFP genome did not enhance rAAV2 titer. It might imply that other than genome amplification, insufficient VP proteins abundance might be another limiting factor for rAAV2 production in CHO-K1 cells.

Table 1. Summary of Transfection Strategies.

Stable Cell Pool	Helper Module	Total DNA (1.25 ug)	mRNA Transposase (1.25 ug)
PoolB1	pEB1	GM:PM:RM:HM = 2:1:1:1	1.25 uL
PoolB2		GM:PM:RM:HM = 1:1:1:1	1.25 uL
PoolAB1	pTEAB1	GM:PM:RM:HM = 2:1:1:1	1.25 uL

PoolAB2		GM:PM:RM:HM = 1:1:1:1	1.25 uL

Having shown that complementing E1B with E1A had a positive effect on rAAV2 productivity, at least in the case of transient transfection results, we proceeded to integrate GM, PM, RM, and either pTEAB1 or pEB1 into CHO-K1, with increased GM proportion in transfection with a GM:RM:PM:HM ratio of 2:1:1:1 as compared to the control of 1:1:1:1 (Table 1). For each ratio, the two HM, with E1A or with E1A and E1B were used. Therefore, a total of four cell pools were created.

Move over, the selective markers for the genome and packaging module were increased to favor the transfectant having higher copy numbers. Although previous selective marker was sufficient for killing numbers transfected CHO-K1 cells in two days, it may allow for the survival of clones with low copy number integration. The concentration of puromycin was increased from 8 μg/mL to 50 μg/mL, and the concentration of blasticidin was tripled, increasing from 10 μg/mL to 30 μg/mL. CHO-K1 cells were transfected with GM, RM, PM and HM cultured for three days before subjected to antibiotic selection for two weeks. During the two weeks of selection, medium exchange was performed every five days. About 80% and 90% cells were killed during selection. Three cell pools, poolEB2, poolEAB1 and poolEAB2, were obtained. No surviving cell pool of pEB1 transfectant was obtained.

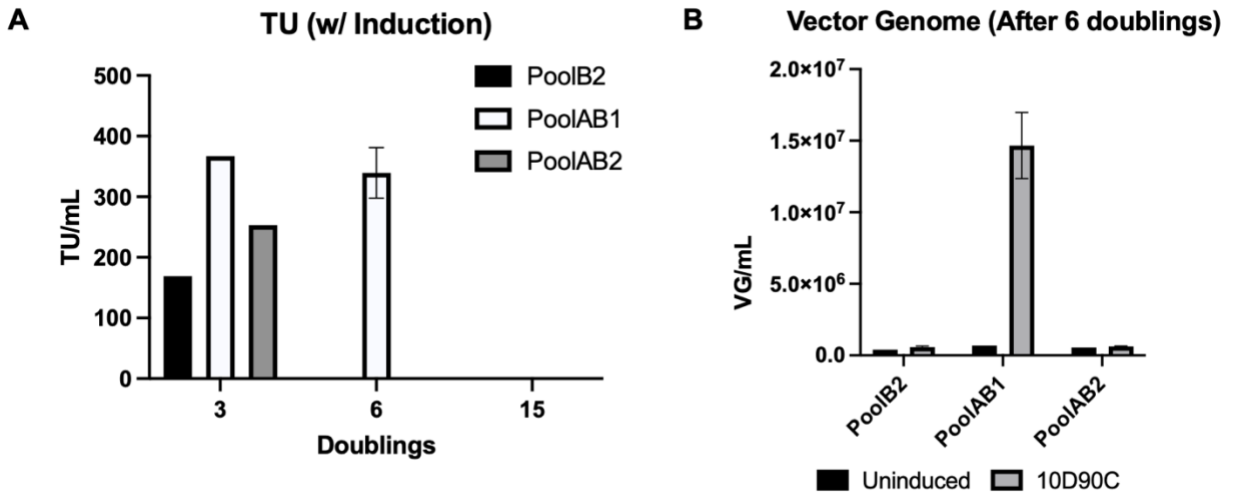

Figure 13. Transducing titer and physical titer of three stable cell pools. (A) Transducing titers of three cell pools at 3, 6 and 15 population doublings were measured by the assay cell line RM4 by counting the GFP-positive cells from twelve images. (B) Physical titers of three cell pools at 6 population doublings after six doublings were measured by qPCR. Data represent mean and standard deviation of triplicate qPCR wells.

The titers in transducing unit and vector genome copy were examined after two weeks of selection. All cell pools produced low levels of infectious rAAV2 particles (Figure 13-A). The transducing unit titers for PoolB2, PoolAB1, PoolAB2 were 1.6 x 10^2 TU/mL, 3.7 x 10^2 TU/mL, and 2.5 x 10^2 TU/mL. However, after 6 doublings, PoolB2 and PoolAB2 lost their productivity, while cell pool PoolAB1 maintained similar titer. Measurement of vector genome titer using qPCR gave the same conclusion. After 6 doublings, cycle differences between uninduced and induced samples from PoolB2 and PoolAB2 were not significant. For PoolAB1, ~3 cycle differences were observed between uninduced and induced conditions, evidenced an increase in viral full particle number upon induction (Figure 13-B).

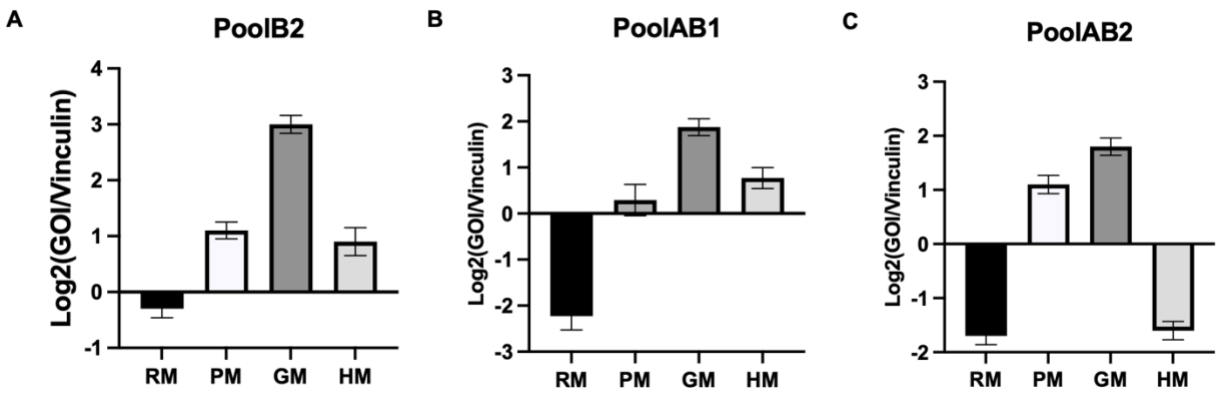

Figure 14. Copy number of integrated GM, PM, RM, and HM of three cell pools, PoolB2 (A), PoolAB1 (B), and PoolAB2 (C). Data represent mean and standard deviation of triplicate qPCR wells.

Integrated copy numbers of four modules for each cell pool were examined by qPCR. In general, RM was the lowest among three cell pools, and GM and PM were the highest and second highest. For cell pool PoolEB2, ~2 copies of RM, ~4 copies of PM, and ~16 copies of GM were integrated into the host cell genome. For cell pool PoolAB1, ~1 copy of RM, ~2 to 3 copies of PM, and ~8 copies of GM were integrated into the host cell genome. For cell pool PoolAB2, ~1 copy of RM, ~4 copies of PM, and ~8 copies of GM were integrated into the host cell genome (Figure 14). Compared to the genomic profile of the cell pool from first attempt (Figure 7), integrated copy numbers of PM and GM were higher this time in all three cell pools, which was likely a result of increased selection stringency for PM and GM. For cell pool PoolAB1 and PoolAB2, their integrated copy numbers of GM were similar (~8 copies), despite two ratios of GM:PM:RM:HM were used for module transfection and integration. This indicated that solely increasing GM ratio in the lipid complex for transfection hardly affect its final integrated copy number (Figure 14).

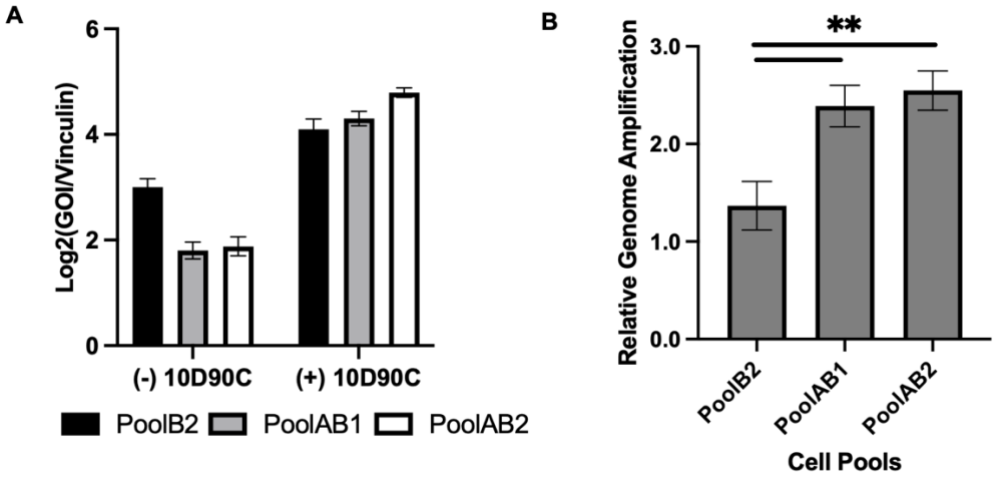

Figure 15. Copy numbers of total intracellular genomes (packaged and unpackaged) of three stable cell pools. Data represent mean and standard deviation of triplicate qPCR wells. For B, *: $p < 0.05$, **: $p < 0.01$, ***: $p < 0.001$ as determined by an unpaired, two-tailed, two-sample t-test.

Genome amplification for three cell pools was quantified. For cell pool PoolB2 with only E1B, intracellular genome before and after induction amplified ~1.2 fold. For cell pools PoolAB1 and PoolAB2 which integrated both E1A and E1B genes, intracellular genome amplified ~2.2 folds before and after induction (Figure 15-A). A two-tail t-test showed that these differences between PoolB2 and PoolAB1 or PoolB2 and PoolAB2 were significant, consistent with the notice that E1A enhanced genome amplification (Figure 15-B).

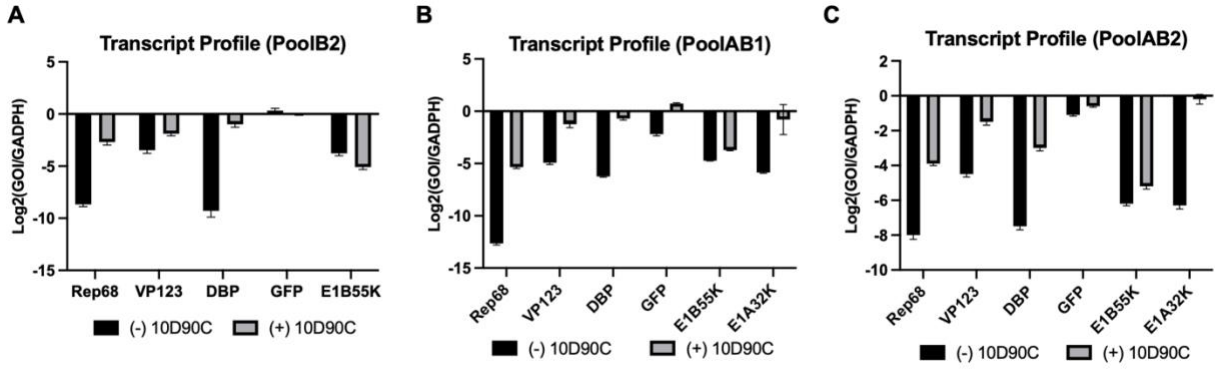

Figure 16. Transcript profiles of three cell pools before induction (-10D90C) and 72 hours after induction (+10D90C). Data represent mean and standard deviation of triplicate qPCR wells.

At the transcription level, four viral genes, Rep68, VP123, DBP, and GFP, from three cell pools showed increase in the level of mRNA after induction. Compared to PoolB2, GFP transcript of cell pool PoolAB1 and PoolAB2 showed higher folds of increasing after induction, validating the conclusion that E1A enhanced genome amplification. Cell pools PoolAB1 and PoolAB2 showed increase E1A transcript after induction, confirmed successful integration of four synthetic modules into the host genome (Figure 16). Compared to the producer clone GX2, Rep68, GFP and DBP transcripts in cell pool PoolAB2 were 2 to 4 folds lower, but the VP123 transcript was comparable. For cell pool PoolB2 and poolAB1, the DBP and GFP transcripts were 4 folds lower, but Rep68 and VP123 transcripts were comparable (Min Lu, personal communication, 2023).

3.1 Isolation of Cell Clones.

A

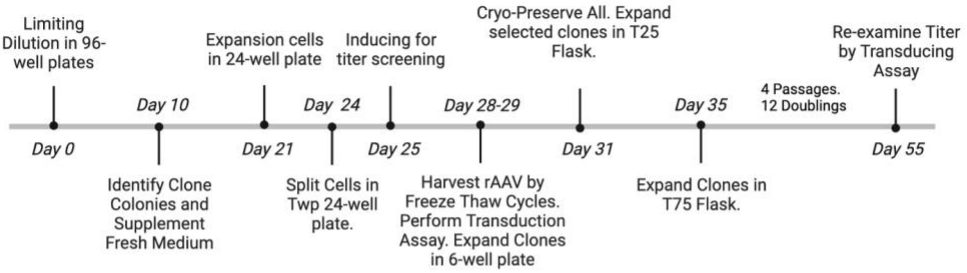

B

# Isolated Clones	**81**
# Producer Clones	**1**
Clone Titer (TU/mL) Before 12 Doublings	$1.43 \pm 0.60 * 10^3$
Clone Titer (TU/mL) After 12 Doublings	**Undetectable**

C

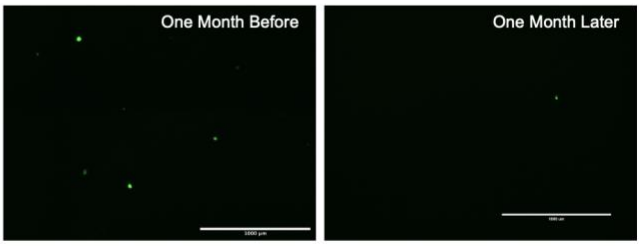

Figure 17. (A) Timeline of rAAV2 producer cell line screening. (B) Number of isolated clones and its virus titer. (C) GFP fluorescence images of RM4 assay cells at 48 h after being transduced with rAAV2-GFP in the clone cell lysate.

While evaluating pool PoolAB1 within 6 doublings, we conducted limiting dilution on PoolAB1 to isolate single cell clones in 96-well-plate according to the sketched timeline (Figure 17). PoolAB1 cells were harvested from T25 flask and pre-diluted to 8 cells/mL with fresh selection medium. About 100 μL cell suspension was added into each well of a 96-well plate. In total, we seeded 20 96-well plates. All 20 96-well plates were placed in CO_2 incubator for outgrowth. After 10 days, we scanned through each 96-well plate using light microscopy and identified growing single cell colonies. These colonies were grown for another 11 days and cells were split into two 24-well plates when becoming confluent. One of the 24 well plate was used for further expansion of cell clones, and cells from the other plate were induced by 10D90C to examine their titer by the RM4 assay cell line. In total, 81 clones were isolated and tested. Similar to previous attempt, most of the isolated clones were unable to produce infectious rAAV particles. Eventually, one producer clone, C18, showed productivity during initial screening. Clone C18 was able to produce 1.43 x 10^3 TU/mL during the initial screening. We expanded clone C18 in T75 flask for 12 doublings. However, after 12 doubling, C18 was unable to produce any infectious rAAV particles, using the assay cell line (Figure 17).

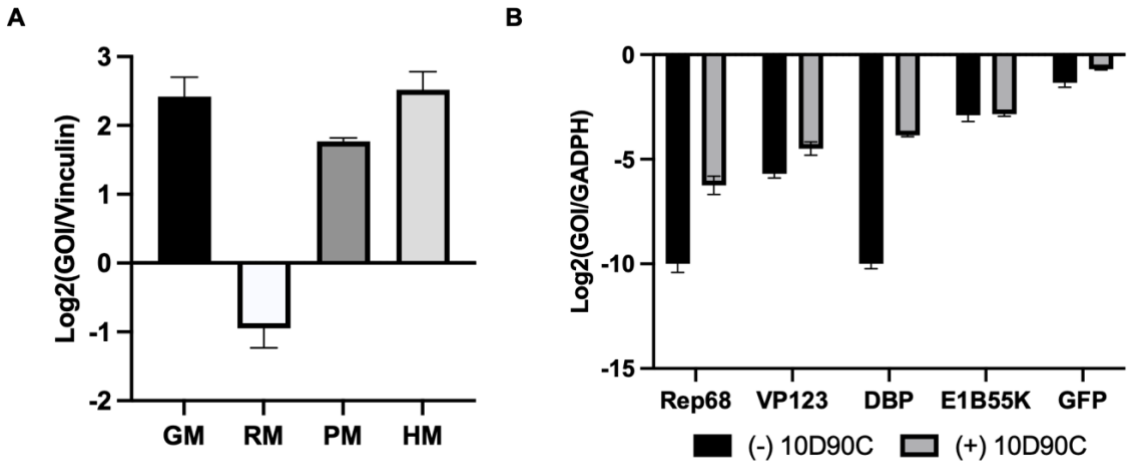

Figure 18. Integrated copy number and transcript profiles of cell clone C18. (A) Integrated copy numbers of GM, RM, PM and HM. (B) Transcript level of viral genes of cell clone C18 before and after induction by dox and cumate. Data represent mean and standard deviation of triplicate qPCR wells.

Copy profile of different modules of Clone C18 was similar to results from cell pool. The integrated copy numbers of GM, PM, and HM were ~8 copies/cell. For RM, the copy number of RM was low, about ~1 copy/cell (Figure 18-A).

Transcript profile of clone C18 after 12 doublings was quantified before and after induction. Transcript of GFP was highly expressed and was slightly increased ~2 cycle upon induction. Transcript levels of DBP and Rep68 increased ~5 folds upon induction, but their expression was still ~5 folds lower than GADPH. Before induction, VP1/2/3 transcript was five cycles lower than GADPH and hardly increased upon induction. This was a strange phenomenon considering about 8 copies of packaging module was integrated into the host cell genome. This indicates that packaging module was not transcriptionally active, or mRNA transcripts were degraded intracellularly. A low level of genome amplification was observation, evidenced by an insignificant increase in GFP transcript level after induction (Figure 18-B).

3.2 Cap Overexpression Enhanced Stable Cell Pool Titer.

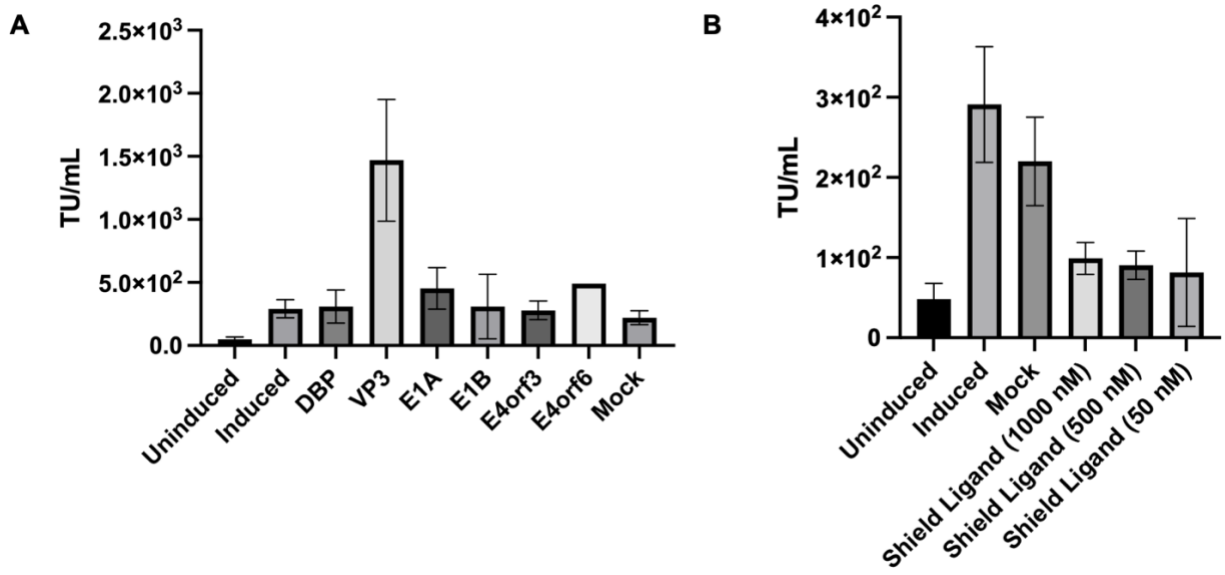

Figure 19. (A) Transducing titer of rAAV2 obtained through the cell pool PoolAB1 transiently transfected with viral genes. (B) Transducing titer of rAAV from cell pool PoolAB1 with 1000, 500, and 50 nM of shield-1 ligand along with inducer with 10D90C. Data represent mean and standard deviation of three independent replicates.

Cell pool PoolAB1 was transiently transfected with six plasmids of viral genes to assess each's ability of increasing rAAV2 titers. This list of genes was selected based on the observation and postulation that genome amplification and capsid protein abundance was constraining rAAV2 production. Viral proteins DBP and E1A would facilitate rAAV2 genome amplification. Protein VP3 was the major component of rAAV2 capsids. Proteins E1B and E4orf6 facilitates export AAV2 mRNA from the nucleus. Protein E4orf3 was also included because it was one of the E4 gene-encoded isoforms, and the complete coding region of E4 gene was included in one of the triple transfection plasmids.

PoolAB1 cells were transfected with one of the six plasmids and induced at the same time. Virus titers of six transfected samples were evaluated by the RM4 assay cell line and compared to the uninduced and induced samples without transfection. To exclude cofounding effects of

transfection reagents, one mock group of PoolAB1 cells with added transfection reagents under induced condition was included. Without transfection, the induced cell pool PoolAB1 could produce 3 x 10^2 TU/mL, which was similar to the virus titers of five transfected samples, DBP, E1A, E1B, E4orf3, or E4orf6. The mock group produced 2 x 10^2 TU/mL. This difference between the two samples was non-significant. What was worth noting was that overexpression of protein VP3 in PoolAB1 cells produced 1.5 x 10^3 TU/mL, 5 folds more than the induced sample (Figure 19-A).

Rep68 was linked with a destabilization domain (DD) to control potential cytotoxicity from leaky expression. Proteins tagged with DD domain would undergo ubiquitin-mediated degradation, but it could be stabilized by the addition of a ligand, Shield-1. Therefore, cells were induced and added with three concentrations of shield1 ligand (1000 nM, 500 nM, 50 nM) to test if stabilizing Rep68 would improve virus titer. Cells that added with three concentrations of shield1 ligand yielded similar titer, ~1 x 10^2 TU/mL, which was three folds lower than the induction-only sample (Figure 19-B).

4 Concluding Remarks

This thesis set out to explore the feasibility of generating infectious rAAV2 vectors using Chinese hamster ovary (CHO) cells. Employing transient transfection, CHO-K1 cells were furnished with three synthetic modules alongside Ad5 E1A and E1B, culminating in the production of infectious rAAV2 vectors at a concentration of 2.0 x 10^5 TU/mL. However, in comparison to both the triple transfection method and the rAAV2 producer cell line derived from HEK293, the overall yield in CHO-K1 cells was notably lower, ranging from 1,000 to 10,000 times. Incorporating insights gleaned from qPCR and western blotting, we successfully pinpointed

potential bottleneck events that curtailed rAAV2 production within CHO-K1 cells. Chief among these was the observation that CHO-K1 cells exhibited limited support for significant rAAV2 genome amplification upon induction. Specifically, the rAAV2 genome experienced a mere 2-fold increase in amplification to 8 copies/cells upon induction within CHO-K1 cells, in contrast to a synthetic cell line GX2 derived from the HEK293 cells where amplification reached up to 15-fold to 9.8×10^4 copies/cells.

Copy numbers of the four synthetic modules within the CHO-K1 host genome were observed to be lower compared to those in the GX2 cell line, potentially contributing to the observed low genome amplification. Thus, it becomes imperative to optimize the strategies for transfection and antibiotic selection in future studies. In the current construct, all antibiotic resistance genes were under the control of the PGK promoter, a strong constitutive promoter in mammalian cells. One potential avenue involves replacing the PGK promoter with a less strong promoters within mammalian cells, thereby fostering the selection of transfectants with higher copy numbers of transgenes even at lower antibiotic concentrations. Another approach entails the utilization of weak internal IRES sites to link the expression of viral genes with antibiotic resistance. This strategic maneuver aims to establish a robust correlation between transgene expression and antibiotic resistance, thereby refining the selection process.

Another possible limiting factor in rAAV2 production within CHO-K1 cells was the expression of capsid proteins. This conclusion was supported by the observation that augmenting VP3 expression in the stable cell pool led to a notable threefold enhancement in rAAV2 titer. Additionally, when the three synthetic modules were overexpressed in CHO-K1 cells, the relative expression of VP3 was lower than that of the loading control, GAPDH, while VP1 and VP2

proteins undetected in the western blotting. In contrast, in triple transfection plasmids of HEK293 cells, VP3 protein expression was at a comparable level as GAPDH, and VP1 and VP2 protein bands were distinctly identifiable. The underlying cause for low capsid protein expression in transient transfection of CHO-K1 cells remain unclear.

CHO cells are the prevailing cells used in therapeutic protein production. The commercial value of CHO produced therapeutic protein exceeds USD$100 billion. Included in the CHO product list is viral protein for immunization applications, such as that for respiratory syncytial virus. Conspicuously missing from that list is virus for vaccine and gene delivery vector applications. This absence of virus product may reflect their non-permissiveness for virus replication and hint at the possibility that viral genome replication triggered antiviral response leading in CHO cells. Host cell antiviral response has been reported to affect the productivity of virus. Through transcriptome analysis of a MDCK cell variant which had a higher influenza virus productivity, it was found that a diminished host antiviral response in the variant contributed to the high productivity (Ye et al., 2021). In another study using a similar synthetic modular system to produce influenza virus (Phan, 2021) it was found that the synthetic cells developed elevated antiviral response which was attributed to the low productivity of the synthetic cells. The duration of constructing the synthetic CHO cell line, from transfection, cell pool, single cell cloning to characterization, is long and giving plenty of time for cells to develop antiviral responses as well as to reduce the expression level of cytotoxic elements (such as Rep68). In future research a strategic focus could involve systematically characterizing the changes in signaling pathways and antiviral responses within CHO-K1 cells upon virus replication. This could be achieved through comprehensive transcriptomic and proteomic analyses.

In conclusion, my study adopted a synthetic biology approach to showcase that CHO-K1 cells can be transiently transfected or stably engineered to produce rAAV2 vector. However, the productivity even in transient transfection of CHO cells was two orders of magnitude lower than that seen in HEK293 cell. HEK293 derived GX2 cells constructed with identical modules yielded also orders of magnitude higher titers. The gap in productivity between CHO and HEK293 could be narrowed somewhat by boosting helper functions of E1B alongside an inducible E1A component. The resulting cell pool demonstrated the ability to generate transducible rAAV2 vectors upon induction. While my work documented a significant stride in exploring an innovative rAAV manufacturing tool and demonstrated the potential of synthetic biology in CHO cells, it also showed the challenges in making CHO cell as a host cell line for viral products.

Addendum: Exploring helper viruses for rAAV2 production system in CHO-K1

1 Fiber-Modified Ad5-RGD Adenovirus Infection of CHO Cell Pool

The Ad5-RGD virus was a kind donation from Professor Masato Yamamoto who is Eugene C. and Gail V. Sit Chair in Pancreatic and Gastrointestinal Cancer Research Vice-Chair of Surgical Science at the University of Minnesota Twin Cities Medical School. We thank him for his helpful discussion and support.

Human adenovirus virus 5 (Ad5), a double-stranded DNA virus, is one of the most commonly used helper viruses for AAV co-infection. The helper genes and their molecular mechanisms involved in AAV replication cycle have been characterized. Our investigation aimed to determine whether Ad5 infection of CHO-K1 cell would enhance the rAAV2 virus production and facilitate the identification of additional helper genes. In this regard, we introduced an Ad5 mutant, Ad5-RGD, to the CHO-K1 cell pools. This choice was driven by the limited entry of wildtype Ad5 (wtAd5) into CHO-K1 cells (Wang & Bergelson, 1999).

Ad5 viral capsid is formed by the major capsid protein hexon in an icosahedral shape with 20 triangular faces. A fiber was bound to another capsid protein penton base and elongated from the viral capsid. An Arg-Gly-Asp (RGD) motif is embedded within the penton base. Ad5 initiates the first step of viral entry by binding of its fibers to the coxsackievirus and adenovirus receptor (CAR). Following the binding of Ad5 fibers and CAR receptors, the RGD peptide interacts with integrins on cellular surface and mediates virus entry (Zhang & Bergelson, 2005). Because the CHO-K1 cell line lacks the CAR receptor, the low-affinity binding between wtAd5 and cells limits virus entry. The Ad5-RGD virus had an RGD-4C sequence in its fiber sequence. This modification improved virus-cell binding affinity and enabled CAR-independent entry as RGD motifs were recognized by cellular integrins. Compared to the wtAd5, Ad5-RGD had enhanced infectivity toward CAR-negative cells, including CHO-K1 cells (Davydova et al., 2004).

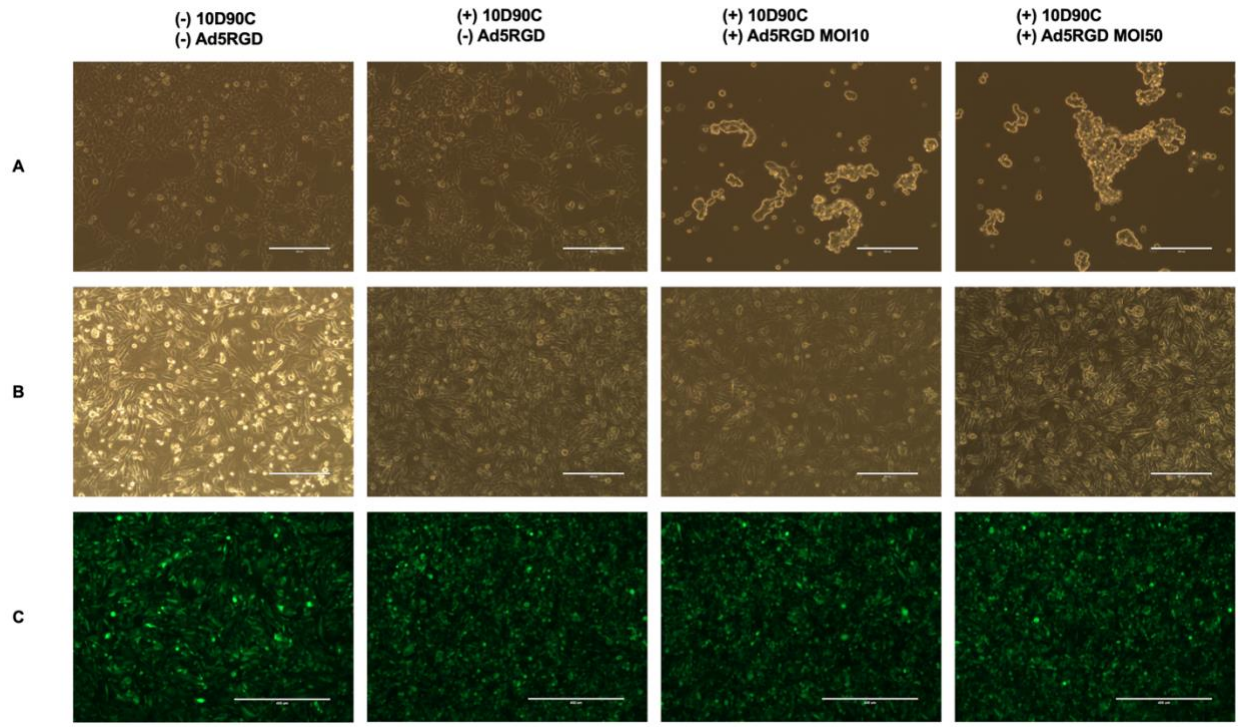

Figure 20. Morphology of HEK293 (A) CHO-tri cell pool (B) and GFP fluorescence images of CHO-tri cell pool (C) at 48 hours after infected with Ad5-RGD (MOI10 or MOI50).

HEK293 and CHO-tri cell pools were plated in 6-well plates at a density of 7.8 x 10^4 cells/cm^2 one day prior to infection and induction. The CHO-tri cell pool was a pooled population which had previously been engineered to have GM, PM, and RM integrated into the genome as described in materials and methods. The CHO-tri cell pool was induced with 10D90C and infected with Ad5-RGD at an MOI of 5 or 10. The negative control groups were HEK293 cells and CHO-GRP which were uninduced and without Ad5-RGD infection. Infection of HEK293 cells with Ad5-RGD was used as the positive control group. Following infection, CHO-K1 cell pools were harvested at 48- or 72-hours post-infection (hpi) for the extraction of cellular gDNA and RNA.

In contrast to non-infected cells, noticeable alterations in cell morphology among infected HEK293 cells became apparent at 24 hours post-infection (hpi). By the 48-hour mark, most of the

infected cells had assumed a rounded and swollen appearance, progressing into apoptosis and exhibiting the distinctive cytopathic effects (CPE) typically associated with adenovirus infection (Figure 20). In contrast, the infected CHO-tri cell pools had no discernible changes in its morphology at the 48-hour post-infection time point its un-infected and induced counterpart. Both maintained a healthy, elongated form. Examination under a green fluorescence microscope revealed that the GFP signals of the CHO-tri cell pools remained unaffected by the Ad5-RGD infection.

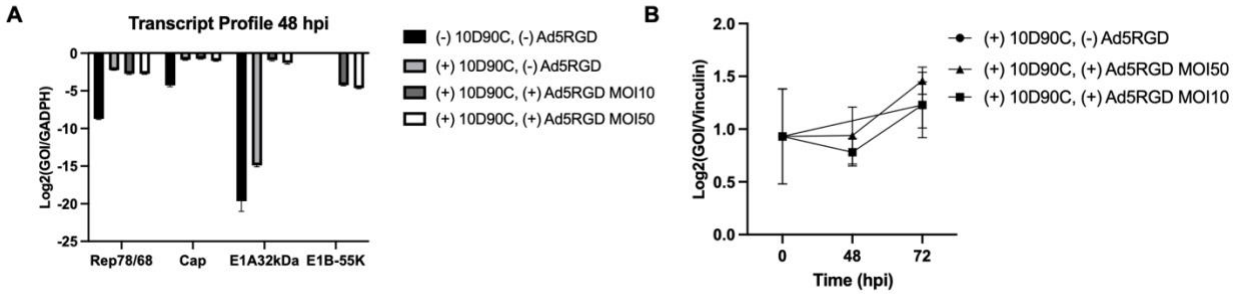

Figure 21. (A) Transcript level of Ad5 and AAV viral genes in Ad5-RGD-uninfected or -infected CHO tri cell pool under uninduced or induced conditions. (B) Total intracellular genomes (packaged and unpackaged) in induced- or uninduced- and Ad5-RGD-infected or -uninfected CHO tri cell pool. Data represents mean and standard deviation of triplicate qPCR wells.

The transcript profile analysis revealed increased transcript levels of E1B55K and E1A genes within the CHO-tri cell pool following infection with Ad5-RGD (Figure 21). In the absence of Ad5-RGD infection, E1A and E1B-55K transcript levels remained undetectable. Following Ad5-RGD infection, the transcript levels of E1A and E1B-55K were found to be 1-2 times lower than that of GAPDH, confirming the successful entry of Ad5-RGD viral particles and transcription of viral genes. However, the difference in fold genome amplification between the infected and

non-infected cell pools was nearly negligible. Notably, Ad5-RGD infection did not contribute to an increased viral genome amplification within the cell pool.

2 Frog Virus 3 (FV3) infection of CHO Cells

In addition to the adenovirus family, various families of DNA viruses have been identified as facilitators of AAV replication, including *Herpesviridae (Weindler & Heilbronn, 1991)*, papillomaviruses (Walz et al., 1997), bocaviruses (Wang et al., 2017), and vaccinia virus (Schlehofer et al., 1986). Notably, studies have revealed that AAV replication can be initiated in vitro even without the presence of a helper virus through the application of the carcinogen, N-methyl-N'-nitro-N-nitrosoguanidine (MNNG) (Yalkinoglu et al., 1988). These studies have suggested that AAV replication occurs under conditions of substantial alteration within the intercellular environment. Given that Ad5 is unable to replicate within CHO cell lines (Berting et al., 2010), we hypothesized that Ad5 infection of CHO-K1 cells does not elicit sufficient intracellular environmental changes for AAV replication. Consequently, Ad5 might not offer sufficient helper functions in this context. We hence set out to identify a double-strand DNA (dsDNA) virus capable of infecting and replicating within CHO-K1 cells, potentially introducing cytopathic response or other novel helper functions conducive to AAV replication.

Several literatures reported frog virus 3 (FV3) could infection and replication in CHO-K1 (Goorha, 1981) (Drillien et al., 1978). Frog virus 3 (FV3) is a member of the *Iridoviridae* virus family. Viruses from this family primarily infect cold-blooded vertebrates, including reptiles, bony fish, and amphibians. The genome of FV3 is a large dsDNA and its length varies from 105-212 kbp. The diameter of viral particle ranges from 120-202 nm (Chinchar et al., 2011). Comparative genomic analysis showed that its genome contained 98 potential nonoverlapping open reading

frames (Tan et al., 2004) and could encode 92-211 putative proteins (Chinchar et al., 2011). The most permissive temperature for FV3 is 29 °C. At 37 °C, viral early proteins are expressed but multiplication is limited (Lopez et al., 1986). Under 29 °C, FV3 is able to amplify 100 folds within CHO-K1 cells within 18 hours (Drillien et al., 1978).

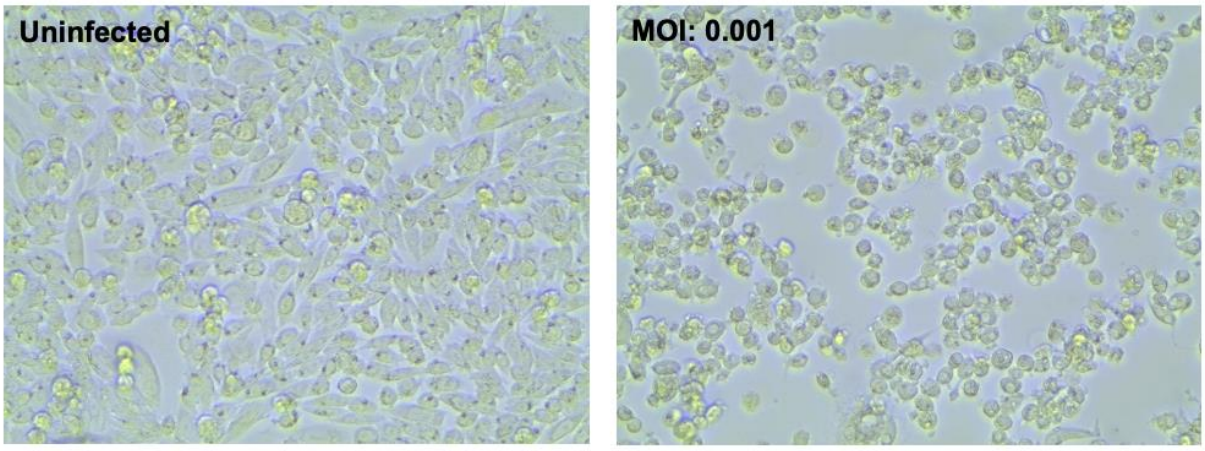

Figure 22. Morphology of CHO-K1 cells under 30 °C at 72 hours after infected with FV3 (MOI 0.001).

We procured FV3 from ATCC. Our objective was to assess the impact of FV3 infection on CHO-K1 cells, especially potential cytopathic effects, on CHO-K1 cells. CHO-K1 cells were subjected to FV3 inoculation at a multiplicity of infection (MOI) of 0.001. Subsequently, both infected and uninfected cell groups were incubated at 30 °C for a duration of 72 hours. Notably, discernible differences in cell morphology between uninfected and infected CHO-K1 cells became evident starting at 48 hours post-infection (hpi). Under microscopic observation, uninfected CHO-K1 cells presented as elongated and transparent. Conversely, infected CHO-K1 cells exhibited a shift towards rounding and detachment from the culture plate. These observed changes in morphology strongly suggest that the CHO-K1 cells were undergoing apoptosis, possibly as a consequence of FV3 infection (Figure 22).

We tested whether FV3 could provide sufficient helper functions for AAV replication by coinfecting of CHO-K1 with FV3 and wtAAV2. To establish control groups, CHO-K1 cells were separately exposed to wtAAV2 at an MOI of 100 or FV3 at an MOI of 10. The test groups were CHO-K1 cell co-infected with FV3 and wtAAV2 at MOIs of 1 and 100 respectively, or 10 and 100 respectively. Recognizing that the optimal growth temperature for CHO-K1 is 37 °C while the permissive temperature for FV3 is 29 °C, we examined four distinct temperature scenarios: CHO-K1 cells were initially seeded under 37 °C for 24 hours prior to infection. In the first two cases, after virus inoculation, CHO-K1 cells were moved under temperature at either 30 or 37 °C for a duration of 72 hours. In the third and fourth case, cells were incubated under 30 or 37 °C for the initial 24 hours, followed infection and a shift to 37 or to 30 °C for the subsequent 48 hours. At 72 hours post-infection (hpi), CHO-K1 cells were harvested, and the physical virus titer was quantified using qPCR.

Table 2. Cycle numbers (Ct) from titration of recombinant Adeno-Associated Virus (rAAV) genome copy number using qPCR. The physical titer of wtAAV2 was probed by primers against AAV2 ITRs. Data represents mean and standard deviation of triplicate qPCR wells.

	AAV2, MOI100	**FV3, MOI10**	**AAV2/FV3, MOI100/1**	**AAV2/FV3, MOI100/10**	**AAV2/FV3, MOI100/10**	**No Infection**
30 (3 Days)	29.6±0.2	33.8±0.3	31.6±0.1	33.1±0.2	31.4±0.0	32.2±0.2
37 (3 Days)	29.9±0.1	35.1±0.5	31.7±0.1	31.2±0.0	29.2±0.0	31.1±0.1
30 (Day 1) 37 (Day 2-3)	29.6±0.1	33.4±0.2	31.7±0.1	32.9±0.1	26.8±0.1	32.4±0.2
37 (Day 1) 30 (Day 2-3)	29.2±0.2	30.7±0.2	29.7±0.2	27.5±0.1	31.1±0.0	33.6±0.2

No significant increase in physical titer was observed when FV3 was coinfected with wtAAV2 (Table 2). The average cycle number for the wtAAV2-infected group across four

temperature profiles was 29, which is 4-5 cycles higher than both the FV3-infected group and the no-infection group. This difference indicates the successful transduction of CHO-K1 cells by wtAAV2. In the coinfection group, two cycle numbers were slightly elevated compared to the baseline value. However, these results could not be consistently replicated under the same conditions. This outcome strongly implies that FV3 is insufficient to provide complete helper functions for AAV replication in CHO-K1 cells.

Reference

Atchison, R. W., Casto, B. C., & Hammon, W. M. (1965). Adenovirus-Associated Defective Virus Particles. *Science*, *149*(3685), 754-756. https://doi.org/10.1126/science.149.3685.754

Berting, A., Farcet, M. R., & Kreil, T. R. (2010). Virus susceptibility of Chinese hamster ovary (CHO) cells and detection of viral contaminations by adventitious agent testing. *Biotechnol Bioeng*, *106*(4), 598-607. https://doi.org/10.1002/bit.22723

Chadeuf, G., Favre, D., Tessier, J., Provost, N., Nony, P., Kleinschmidt, J., Moullier, P., & Salvetti, A. (2000). Efficient recombinant adeno-associated virus production by a stable rep-cap HeLa cell line correlates with adenovirus-induced amplification of the integrated rep-cap genome [https://doi.org/10.1002/1521-2254(200007/08)2:4<260::AID-JGM111>3.0.CO;2-8]. *The Journal of Gene Medicine*, *2*(4), 260-268. https://doi.org/https://doi.org/10.1002/1521-2254(200007/08)2:4<260::AID-JGM111>3.0.CO;2-8

Chang, L. S., Shi, Y., & Shenk, T. (1989). Adeno-associated virus P5 promoter contains an adenovirus E1A-inducible element and a binding site for the major late transcription factor. *J Virol*, *63*(8), 3479-3488. https://doi.org/10.1128/JVI.63.8.3479-3488.1989

Chinchar, V. G., Yu, K. H., & Jancovich, J. K. (2011). The molecular biology of frog virus 3 and other iridoviruses infecting cold-blooded vertebrates. *Viruses*, *3*(10), 1959-1985. https://doi.org/10.3390/v3101959

Clark, K. R., Voulgaropoulou, F., Fraley, D. M., & Johnson, P. R. (1995). Cell Lines for the Production of Recombinant Adeno-Associated Virus. *Human Gene Therapy*, *6*(10), 1329-1341. https://doi.org/10.1089/hum.1995.6.10-1329

Clément, N., & Grieger, J. C. (2016). Manufacturing of recombinant adeno-associated viral vectors for clinical trials. *Molecular Therapy - Methods & Clinical Development*, *3*, 16002. https://doi.org/https://doi.org/10.1038/mtm.2016.2

Drillien, R., Spehner, D., & Kirn, A. (1978). Host range restriction of vaccinia virus in Chinese hamster ovary cells: relationship to shutoff of protein synthesis. *J Virol*, *28*(3), 843-850. https://doi.org/10.1128/JVI.28.3.843-850.1978

Elmore, Z. C., Patrick Havlik, L., Oh, D. K., Anderson, L., Daaboul, G., Devlin, G. W., Vincent, H. A., & Asokan, A. (2021). The membrane associated accessory protein is an adeno-

associated viral egress factor. *Nat Commun*, *12*(1), 6239. https://doi.org/10.1038/s41467-021-26485-4

Farson, D., Harding, T. C., Tao, L., Liu, J., Powell, S., Vimal, V., Yendluri, S., Koprivnikar, K., Ho, K., Twitty, C., Husak, P., Lin, A., Snyder, R. O., & Donahue, B. A. (2004). Development and characterization of a cell line for large-scale, serum-free production of recombinant adeno-associated viral vectors [https://doi.org/10.1002/jgm.622]. *The Journal of Gene Medicine*, *6*(12), 1369-1381. https://doi.org/https://doi.org/10.1002/jgm.622

Gonçalves, M. A. F. V. (2005). Adeno-associated virus: from defective virus to effective vector. *Virology Journal*, *2*(1), 43. https://doi.org/10.1186/1743-422X-2-43

Goorha, R. (1981). Frog virus 3 requires RNA polymerase II for its replication. *J Virol*, *37*(1), 496-499. https://doi.org/10.1128/JVI.37.1.496-499.1981

Grieger, J. C., Soltys, S. M., & Samulski, R. J. (2016). Production of Recombinant Adeno-associated Virus Vectors Using Suspension HEK293 Cells and Continuous Harvest of Vector From the Culture Media for GMP FIX and FLT1 Clinical Vector. *Mol Ther*, *24*(2), 287-297. https://doi.org/10.1038/mt.2015.187

He, X., Urip, B. A., Zhang, Z., Ngan, C. C., & Feng, B. (2021). Evolving AAV-delivered therapeutics towards ultimate cures. *J Mol Med (Berl)*, *99*(5), 593-617. https://doi.org/10.1007/s00109-020-02034-2

Kim, J. Y., Kim, Y. G., & Lee, G. M. (2012). CHO cells in biotechnology for production of recombinant proteins: current state and further potential. *Appl Microbiol Biotechnol*, *93*(3), 917-930. https://doi.org/10.1007/s00253-011-3758-5

King, J. A., Dubielzig, R., Grimm, D., & Kleinschmidt, J. A. (2001). DNA helicase-mediated packaging of adeno-associated virus type 2 genomes into preformed capsids [https://doi.org/10.1093/emboj/20.12.3282]. *The EMBO Journal*, *20*(12), 3282-3291. https://doi.org/https://doi.org/10.1093/emboj/20.12.3282

Kuriakose, A., Chirmule, N., & Nair, P. (2016). Immunogenicity of Biotherapeutics: Causes and Association with Posttranslational Modifications. *J Immunol Res*, *2016*, 1298473. https://doi.org/10.1155/2016/1298473

Lee, Z., Lu, M., Irfanullah, E., Soukup, M., & Hu, W. S. (2022). Construction of an rAAV Producer Cell Line through Synthetic Biology. *ACS Synth Biol*, *11*(10), 3285-3295. https://doi.org/10.1021/acssynbio.2c00207

Lee, Z., Lu, M., Irfanullah, E., Soukup, M., Schmidt, D., & Hu, W. S. (2023). Development of an Inducible, Replication-Competent Assay Cell Line for Titration of Infectious Recombinant Adeno-Associated Virus Vectors. *Hum Gene Ther*, *34*(3-4), 162-170. https://doi.org/10.1089/hum.2022.001

Lopez, C., Aubertin, A. M., Tondre, L., & Kirn, A. (1986). Thermosensitivity of frog virus 3 genome expression: defect in early transcription. *Virology*, *152*(2), 365-374. https://doi.org/10.1016/0042-6822(86)90139-x

Matsushita, T., Okada, T., Inaba, T., Mizukami, H., Ozawa, K., & Colosi, P. (2004). The adenovirus E1A and E1B19K genes provide a helper function for transfection-based adeno-associated virus vector production. *J Gen Virol*, *85*(Pt 8), 2209-2214. https://doi.org/10.1099/vir.0.79940-0

Mullard, A. (2023). FDA approves first gene therapy for Duchenne muscular dystrophy, despite internal objections. *Nat Rev Drug Discov*, *22*(8), 610. https://doi.org/10.1038/d41573-023-00103-y

Ogden, P. J., Kelsic, E. D., Sinai, S., & Church, G. M. (2019). Comprehensive AAV capsid fitness landscape reveals a viral gene and enables machine-guided design. *Science*, *366*(6469), 1139. https://doi.org/10.1126/science.aaw2900

Phan, T. (2021). *Systems Design and Synthetic Construction of Influenza Virus for Flu Vaccine Application* University of Minnesota]. University of Minnesota. https://hdl.handle.net/11299/225883

Qiao, C., Li, J., Skold, A., Zhang, X., & Xiao, X. (2002). Feasibility of generating adeno-associated virus packaging cell lines containing inducible adenovirus helper genes. *Journal of virology*, *76*(4), 1904-1913. https://doi.org/10.1128/jvi.76.4.1904-1913.2002

Samulski, R. J., & Muzyczka, N. (2014). AAV-Mediated Gene Therapy for Research and Therapeutic Purposes. *Annu Rev Virol*, *1*(1), 427-451. https://doi.org/10.1146/annurev-virology-031413-085355

Schlehofer, J. R., Ehrbar, M., & zur Hausen, H. (1986). Vaccinia virus, herpes simplex virus, and carcinogens induce DNA amplification in a human cell line and support replication of a helpervirus dependent parvovirus. *Virology*, *152*(1), 110-117. https://doi.org/10.1016/0042-6822(86)90376-4

Schmidt, M., Afione, S., & Kotin Robert, M. (2000). Adeno-Associated Virus Type 2 Rep78 Induces Apoptosis through Caspase Activation Independently of p53. *Journal of Virology*, *74*(20), 9441-9450. https://doi.org/10.1128/JVI.74.20.9441-9450.2000

Sonntag, F., Schmidt, K., & Kleinschmidt, J. A. (2010). A viral assembly factor promotes AAV2 capsid formation in the nucleolus. *Proceedings of the National Academy of Sciences of the United States of America*, *107*(22), 10220-10225. https://doi.org/10.1073/pnas.1001673107

Srivastava, A., Mallela, K. M. G., Deorkar, N., & Brophy, G. (2021). Manufacturing Challenges and Rational Formulation Development for AAV Viral Vectors. *Journal of Pharmaceutical Sciences*, *110*(7), 2609-2624. https://doi.org/https://doi.org/10.1016/j.xphs.2021.03.024

Swanson, K. A., Rainho-Tomko, J. N., Williams, Z. P., Lanza, L., Peredelchuk, M., Kishko, M., Pavot, V., Alamares-Sapuay, J., Adhikarla, H., Gupta, S., Chivukula, S., Gallichan, S., Zhang, L., Jackson, N., Yoon, H., Edwards, D., Wei, C. J., & Nabel, G. J. (2020). A respiratory syncytial virus (RSV) F protein nanoparticle vaccine focuses antibody responses to a conserved neutralization domain. *Sci Immunol*, *5*(47). https://doi.org/10.1126/sciimmunol.aba6466

Tan, W. G., Barkman, T. J., Gregory Chinchar, V., & Essani, K. (2004). Comparative genomic analyses of frog virus 3, type species of the genus Ranavirus (family Iridoviridae). *Virology*, *323*(1), 70-84. https://doi.org/10.1016/j.virol.2004.02.019

Tullis Gregory, E., & Shenk, T. (2000). Efficient Replication of Adeno-Associated Virus Type 2 Vectors: a cis-Acting Element outside of the Terminal Repeats and a Minimal Size. *Journal of Virology*, *74*(24), 11511-11521. https://doi.org/10.1128/JVI.74.24.11511-11521.2000

Vachon, V. K., & Conn, G. L. (2016). Adenovirus VA RNA: An essential pro-viral non-coding RNA. *Virus Research*, *212*, 39-52. https://doi.org/https://doi.org/10.1016/j.virusres.2015.06.018

Walz, C., Deprez, A., Dupressoir, T., Durst, M., Rabreau, M., & Schlehofer, J. R. (1997). Interaction of human papillomavirus type 16 and adeno-associated virus type 2 co-infecting human cervical epithelium. *J Gen Virol*, *78 (Pt 6)*, 1441-1452. https://doi.org/10.1099/0022-1317-78-6-1441

Wang, Z., Deng, X., Zou, W., Engelhardt, J. F., Yan, Z., & Qiu, J. (2017). Human Bocavirus 1 Is a Novel Helper for Adeno-associated Virus Replication. *J Virol*, *91*(18). https://doi.org/10.1128/JVI.00710-17

Ward, P., Dean, F. B., O'Donnell, M. E., & Berns, K. I. (1998). Role of the adenovirus DNA-binding protein in in vitro adeno-associated virus DNA replication. *Journal of virology*, *72*(1), 420-427. https://doi.org/10.1128/jvi.72.1.420-427.1998

Weindler, F. W., & Heilbronn, R. (1991). A subset of herpes simplex virus replication genes provides helper functions for productive adeno-associated virus replication. *J Virol*, *65*(5), 2476-2483. https://doi.org/10.1128/JVI.65.5.2476-2483.1991

Weitzman, M. D., Fisher, K. J., & Wilson, J. M. (1996). Recruitment of wild-type and recombinant adeno-associated virus into adenovirus replication centers. *Journal of Virology*, *70*(3), 1845-1854. https://doi.org/10.1128/jvi.70.3.1845-1854.1996

Wu, Z., Yang, H., & Colosi, P. (2010). Effect of Genome Size on AAV Vector Packaging. *Molecular Therapy*, *18*(1), 80-86. https://doi.org/https://doi.org/10.1038/mt.2009.255

Yalkinoglu, A. O., Heilbronn, R., Burkle, A., Schlehofer, J. R., & zur Hausen, H. (1988). DNA amplification of adeno-associated virus as a response to cellular genotoxic stress. *Cancer Res*, *48*(11), 3123-3129. https://www.ncbi.nlm.nih.gov/pubmed/2835153

Ye, Q., Phan, T., Hu, W. S., Liu, X., Fan, L., Tan, W. S., & Zhao, L. (2021). Transcriptomic Characterization Reveals Attributes of High Influenza Virus Productivity in MDCK Cells. *Viruses*, *13*(11). https://doi.org/10.3390/v13112200